



Liquid Crystals

Publication details, including instructions for authors and subscription information:

<http://www.tandfonline.com/loi/tlct20>

Photochromic azobenzene functionalised banana-calamitic dimers and trimers: mesophase behaviour and photo-orientational phenomena

Maria-Gabriela Tamba^{a b}, Alexey Bobrovsky^c, Valery Shibaev^c, Gerhard Pelzl^a, Ute Baumeister^a & Wolfgang Weissflog^a

^a Institut für Chemie, Physikalische Chemie, Martin-Luther-Universität Halle-Wittenberg, Halle, Germany

^b Department of Chemistry, University of Hull, Kingston upon Hull, UK

^c Faculty of Chemistry, Moscow State University, Moscow, Russia

Available online: 22 Nov 2011

To cite this article: Maria-Gabriela Tamba, Alexey Bobrovsky, Valery Shibaev, Gerhard Pelzl, Ute Baumeister & Wolfgang Weissflog (2011): Photochromic azobenzene functionalised banana-calamitic dimers and trimers: mesophase behaviour and photo-orientational phenomena, *Liquid Crystals*, 38:11-12, 1531-1550

To link to this article: <http://dx.doi.org/10.1080/02678292.2011.626084>

PLEASE SCROLL DOWN FOR ARTICLE

Full terms and conditions of use: <http://www.tandfonline.com/page/terms-and-conditions>

This article may be used for research, teaching, and private study purposes. Any substantial or systematic reproduction, redistribution, reselling, loan, sub-licensing, systematic supply, or distribution in any form to anyone is expressly forbidden.

The publisher does not give any warranty express or implied or make any representation that the contents will be complete or accurate or up to date. The accuracy of any instructions, formulae, and drug doses should be independently verified with primary sources. The publisher shall not be liable for any loss, actions, claims, proceedings, demand, or costs or damages whatsoever or howsoever caused arising directly or indirectly in connection with or arising out of the use of this material.

INVITED ARTICLE

Photochromic azobenzene functionalised banana–calamitic dimers and trimers: mesophase behaviour and photo-orientational phenomena

Maria-Gabriela Tamba^{a,b,*}, Alexey Bobrovsky^c, Valery Shibaev^c, Gerhard Pelzl^a, Ute Baumeister^a and Wolfgang Weissflog^a

^a*Institut für Chemie, Physikalische Chemie, Martin-Luther-Universität Halle-Wittenberg, Halle, Germany;* ^b*Department of Chemistry, University of Hull, Kingston upon Hull, UK;* ^c*Faculty of Chemistry, Moscow State University, Moscow, Russia*

(Received 1 August 2011; final version received 19 September 2011)

Azobenzene functionalised banana–calamitic dimers and a novel type of banana–calamitic–banana trimers have been synthesised. Their thermotropic behaviour and the structure of the mesophases have been characterised by differential scanning calorimetry, polarising optical microscopy and X-ray diffractions measurements. Electro-optical studies evidence the polar properties of the smectic phases. A rare anticlinic–synclinic smectic CP (SmCP) phase transition could be proven for two of the twins upon cooling without an electric field although the molecules are not optically active. Remarkably, the phase sequence SmC_a–SmC_s has been observed upon cooling, the inverse sequence to that reported for non-chiral compounds up to now. A comparative study of the photochemical properties of dilute solutions and of thin films of two compounds has been performed. Irradiation with polarised ultra-violet (365 nm) and visible light (473 nm) induces a photo-orientation process of the chromophores in a direction perpendicular to the polarisation plane of the exciting light. For a trimeric compound bearing an azobenzene bridge between both bent-core mesogenic units this process is associated with cycles of the *E*–*Z*–*E* isomerisation of the azobenzene groups followed by rotational diffusion of molecules in the films. For a bis(azobenzene) containing dimer the *E*–*Z* isomerisation in films is strongly suppressed and the photo-induced orientation has a rotational diffusion mechanism.

Keywords: bent-core mesogens; banana-calamitic dimers; banana-calamitic trimers; photo-orientational effect; synclinic-anticlinic SmCP phase transition; electro-optical behaviour

1. Introduction

Azobenzene compounds are materials of interest for different reasons. Due to their rod-like shape, terminally substituted azobenzenes represent one of the oldest classes of liquid crystals forming nematic and smectic phases. Azobenzene moieties can be inserted into discotic, dimeric, oligomeric, and polymeric structures. The combination of azobenzene with a bent-core mesogenic moiety resulting in banana–calamitic dimers, however, has not been described until now. Bent-core mesogens form different types of mesophases, so-called banana phases. The question is what happens if a calamitic azobenzene fragment is covalently linked with a bent-core moiety by means of an aliphatic spacer. This question is not only of importance when concerning the liquid crystalline (LC) behaviour and the structure of the mesophases but also when concerning the photochemical properties. The photo-induced *E*–*Z* isomerisation of the azo group results in a changed molecular shape and can be applied for photo-orientation effects, which are of practical importance. It is well known that the photochemistry depends on the chemical

surrounding of the azo group. In this paper, the synthesis of new banana–calamitic dimers and of a novel type of banana–calamitic–banana trimers containing azobenzene moieties is presented. The LC properties and the photo-orientational behaviour of the new compounds are studied.

Photochromic low-molar mass and polymer systems have attracted a growing interest of many research groups. Such an interest is associated with the possibility of manipulating the molecular shape and the supramolecular structure and the possibility of a wide range of promising applications in photonics, optoelectronics, optical data storage, etc. [1–7].

After the discovery of the photo-orientation phenomena in dye-containing compounds (frequently called Weigert effect [8]) a huge number of publications dealing with the study of similar effects in azobenzene-containing low-molar mass and polymer systems have appeared [9–30]. One of the mechanisms of photo-orientation is based on the photo-induced *E*–*Z* isomerisation of azobenzene chromophores, accompanied by their rotational diffusion and rearrangement so that their long axes are oriented

*Corresponding author. Email: gabiela_tamba@yahoo.com; m.tamba@hull.ac.uk

perpendicular to the electric field vector of the polarised light. More specifically, the probability of photon absorption is proportional to $\cos 2\varphi$, where φ is the angle between the light polarisation and the axis of the transition moment for the azobenzene moiety. Azobenzene groups, which are oriented along the polarisation direction, absorb light with high probability, whereas an absorbance of the groups oriented at 90° to the incident polarisation is much less. Each time a chromophore undergoes the *E*–*Z*–*E* isomerisation cycles; its position varies in a small and random way. Thus, when starting from an initial random angular distribution of chromophores, those oriented along the polarisation direction will absorb and reorient, whereas those oriented perpendicular the polarisation direction do not move. Eventually, most of the chromophores become oriented perpendicular to the polarisation plane. In most cases this process has a cooperative nature and involves non-photochromic fragments in the system.

The majority of the existing publications deal with investigations on the photo-selection and the photo-orientation processes in amorphous and LC polymers of the nematic or smectic type [9–30]. Only a few papers consider photo-orientation processes in low-molar mass amorphous glassy compounds [31–33]. It has been demonstrated that in these systems only small values of photo-induced order parameter and dichroism were achieved (~ 0.004), which are much smaller than those for the azobenzene-containing LC polymers (in the range of 0.3–0.7 [9–30]).

Nowadays, among different types of LC compounds, bent-shaped mesogens have attracted considerable research interest in the field of soft condensed matter. Banana-shaped molecules forming liquid crystals strongly deviate from the classical rod-like or disc-like shape and allow special steric interaction. Due to their bent shape, the molecules can be preferably packed in the bent direction giving rise to long-range correlation of the lateral dipole moments that results in macroscopic polarisation within the smectic layers (designated by P after the symbol of the smectic phase). Depending on the interlayer correlation, ferroelectric and antiferroelectric smectic phases (subscripts F or A after P) can result. If the molecular long axes are arranged perpendicularly to the layers, smectic AP (SmAP_F) or (SmAP_A) phases result. In most cases, the polar packed bent molecules are tilted with respect to the layer normal. Two basic arrangements are possible: synclinic and anticlinic, subscripted by (s) or (a) after C. That means, four types of smectic CP (SmCP) phases are possible: SmC_sP_A , SmC_sP_F , SmC_aP_A and SmC_aP_F . Another point of interest should be stressed: the combination of polar order within the layers and director tilt can lead to supramolecular chirality although the molecules do

not exhibit optical activity. Two of the four SmCP phases exhibit such homochiral states— SmC_sP_F and SmC_aP_A —which mean that the layer chirality is uniform within a macroscopic domain. The relationships between the chemical structure and the mesomorphic properties of the bent-shaped compounds have been investigated extensively. In discussing this connection and the structure of the different B phases (B_1 – B_8 and others) and their physical properties, we refer to some original papers and reviews on banana-shaped liquid crystals [34–41].

Bent-core mesogens usually consist of five or six phenyl units that are connected by linking groups used in liquid crystal chemistry, for example carboxyl or azomethine groups. In most cases, the bend of the molecular long axis results from a 1,3-phenylene connection near to the centre of the molecule. When azo linking groups are inserted between the two phenyl rings, the banana-shaped liquid crystals become sensitive towards light, which is of interest in relation to the present work.

Pioneering work has been done in the field of azo-containing bent-core mesogens by Prasad et al. [42–45]. The first compounds forming electrically switchable and photo-responsive mesophases have also been reported [46]. The authors studied the influence of light action on the phase transition temperatures of these compounds and found that the formation of *Z*-isomers during photo-irradiation results in a small decrease of the phase transitions temperatures (Cr to B_2 phase as well as B_2 phase to the isotropic one). Jakli and Prasad et al. have reported the light-induced changes on the optical and electrical properties [47].

Ros et al. studied the mesophase structure and non-linear optical phenomena in different bent-core compounds with azo and azoxy bonds [48–50]. Measurements of the optical second-harmonic generation have been performed on aligned samples. By changing the molecular design, the second-order susceptibility tensor could be remarkably increased. Irradiation of the samples in the LC state by the polarised light of an argon laser results in only an isothermal transition from the mesophase to the isotropic state. The process is reversible by switching off the light source. No photo-orientation process has been observed. Recently, the same research group reported photo-modulation in the columnar phase formed by supramolecular aggregates, which result by hydrogen bonding between a melamine derivative and an azo-containing bent-core mesogen bearing a free carboxylic group [51].

Light modulation experiments have also been performed using mixtures of bent-core and calamitic liquid crystals. One of the mesogens used was an azo compound. Interesting results concerning

the influence of light on the polarisation of a banana-shaped host compound doped by a rod-like azobenzene substance are described in [52–53]. It was found that the *E*–*Z* photo-isomerisation of the azobenzene molecules, induced by ultraviolet (UV) light, only slightly changes the isotropisation temperatures, but has a significant influence on the spontaneous polarisation and the switching time in the polar phase of the host matrix. In addition, the efficiency of this light induced change of polarisation has been observed to be strongly dependent on the temperature at which the irradiation is carried out. A possible mechanism responsible for the observed phenomenon has been suggested.

The photo-induced reorientation of smectic layers from an alignment perpendicular to the substrate to that parallel to it has been found in similar guest–host mixtures containing a bent-shaped matrix that have been doped by rod-like azobenzene molecules [54].

Lutfor et al. prepared, and studied, new bent-shaped azobenzene monomers. One of these was mixed as a guest with calamitic liquid crystals serving as the host to perform photo-isomerisation studies [55].

Recent papers [55, 56] report on the synthesis of new azobenzene-containing bent-shaped monomers and their photochemical properties in mixtures with calamitic liquid crystals in dilute solution. Kinetics of the forward photo-induced *E*–*Z* isomerisation and thermal back *Z*–*E* isomerisation were studied. An increase in thermal back relaxation time has been found, which could be useful for creation of optical image storage devices.

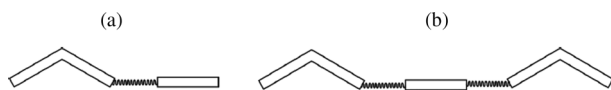
Beside azo group containing bent-core mesogens and/or their mixtures discussed before, the covalent connection of two mesogens by means of a flexible spacer resulting in LC dimers is a further possibility to create photo-sensitive materials. When starting with conventional twin molecules; a lot of symmetric and non-symmetric dimers and trimers containing azobenzene have been reported in the literature [57]. In a few cases, two rod-like mesogens are laterally connected by the –N=N– group, giving H-shaped twin molecules, which are of interest due to their second order non-linear optics [58–60]. However, both calamitic mesogenic units are terminally linked together. Two azobenzene moieties can be connected to each other, for example, to study the spacer parity of the photo-induced effects [61]. Twin molecules having a relatively short odd-numbered spacer can be reminiscent of the banana-shaped mesogens with respect to their properties. Choi et al. found a circular-polarisation-induced enantiomeric excess in such a bent azobenzene dimer [62]. Photochemically induced smectic–cholesteric phase transitions have been reported by Mallia et al.

[63, 64] for twin molecules consisting of an azobenzene unit linked to cholesterol by a spacer. Three mesogenic moieties can also be connected in different way [65–68]. Centrosymmetric azobenzene substituted trimers appear to be candidates for stable holographic volume gratings [66]. The numbers of papers related to dimeric and trimeric liquid crystals is very high, therefore only several selected examples could be cited here.

Dimers consisting of a bent-core and a calamitic mesogenic unit and bearing an azo group in any position have not been reported until now. If two bent-core moieties are terminally linked together, the parity of the spacer strongly influences the LC behaviour. Mostly, “banana phases” have been found [69–75]. Banana–calamitic dimers are of topical interest because “banana phases” and “calamitic phases” can exist for the same compound. Nematic and smectic phases formed by bent-core mesogens can exhibit unusual physical properties, e.g. the formation of chiral domains even though the molecules are not chiral and have unusual pattern formations upon applying an electric field [76, 77]. Several bent-core mesogens could be candidates for biaxial nematic phases [78]. Few banana–calamitic dimers have been reported until now. Yelamagad et al. observed a latently biaxial nematic phase for a compound consisting of a five-ring bent-core mesogenic unit linked to cyanobiphenyl by the means of flexible spacers [79, 80]. The connection of a banana-shaped moiety to cholesterol results in materials showing broad existence ranges of a blue phase [81, 82]. Recently, Lee et al. have investigated a dimer containing cyanobiphenyl and a four-ring bent-core unit, which is similar to a hockey stick-shaped fragment. The nematic phase does not exhibit biaxiality but an anchoring transition behaviour [83]. In 2006 we reported three banana–calamitic dimers. The dimers exhibit exciting physical properties like field-induced texture transition, the occurrence of a metastable biaxial nematic state, and the formation of an unusual electro-convection pattern [84–87]. Following on from this, we started systematic studies to understand the relationships between the chemical structure, LC behaviour and physical properties [88].

Finally, it should be noted that the attachment of two cyanobiphenyl fragments to both the legs of the bent-core unit yields a calamitic–banana–calamitic trimer, which exhibits a typical nematic phase without any unusual properties [89]. Bisoyi et al. have published a second type of trimeric compound. In these compounds, which do not exhibit a mesophase, two discotic triphenylene moieties are linked to both terminal ends of the central five-ring bent-core unit [90].

In this paper, we report on azobenzene functionalised banana–calamitic dimers, see Scheme 1(a). Furthermore, trimers consisting of two bent-core



Scheme 1. Schematic of the banana-calamitic dimers (a) and the banana-calamitic-banana trimers (b) that were studied. The rod-like part represents an azobenzene fragment and the mesogenic units are connected by flexible spacers.

mesogens linked by an azobenzene bridge were synthesised. These trimers represent a novel type of oligomer containing two banana-shaped mesogenic units together with a calamitic one, as shown in Scheme 1(b).

After preparation and characterisation of the compounds, the phase structures were investigated by optical polarising microscopy and X-ray diffraction (XRD) measurements. Information regarding the polar properties and field-induced effects were obtained by electro-optical studies.

As discussed above, polarised light is a unique tool for manipulating the orientation of the chromophores and the mesogens in azobenzene-containing systems. However, to the best of our knowledge, there are no reports on photo-orientation phenomena in thin solid films of bent-shaped photosensitive substances. Therefore, the goal of our work is the study of photo-optical properties of these new substances in solutions and films. Special attention will be paid to the photo-orientational processes induced under polarised light in thin amorphous films prepared by the spin-coating technique. One member of each series (compounds **1c** and **2d**) was selected for the photochemical studies.

2. Experimental details

2.1 Synthesis

The best way to prepare the compounds under discussion is the connection of a bent-core fragment and a calamitic moiety that are both ω -functionalised. The crucial point is to find the best position for this linking, which allows an effective separation and purification of the final products in high yields.

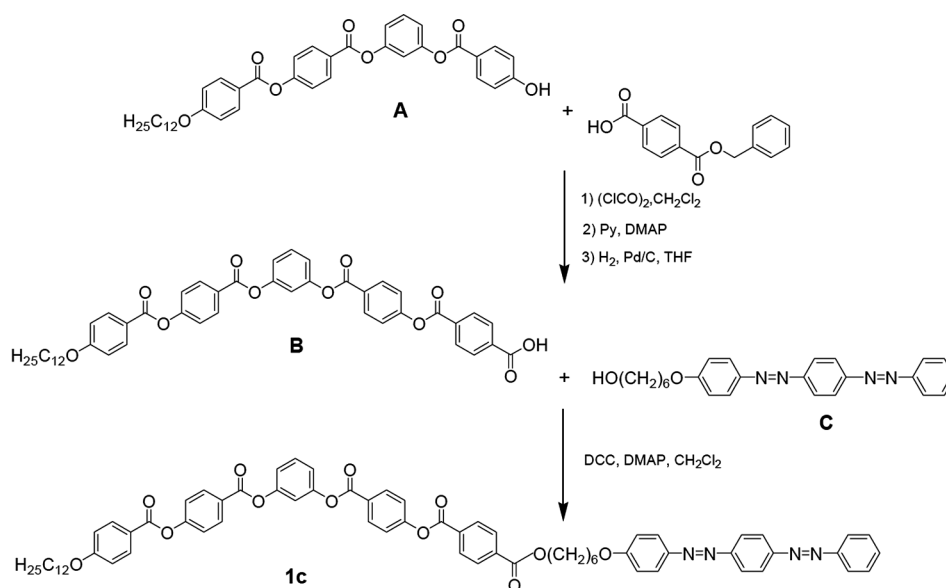
Schemes 2 and 3 show the final steps in the preparation of the banana-calamitic dimer **1c** and the banana-calamitic-banana trimer **2d**. The multi-step reaction to synthesise the five-ring bent-core moiety **B** bearing a carboxylic group in a terminal position is based on the esterification of the four-ring phenol **A** [91] with 4-benzyloxycarbonylbenzoic acid and following de-protection. The synthesis and properties of 4-(ω -hydroxyalkyloxy)bisazobenzenes having different alkylene spacers have been described in [92], and those of the 4,4'-bis(ω -hydroxyalkyloxy)azobenzenes by Rötz et al. [93].

2.1.1 Experimental procedure

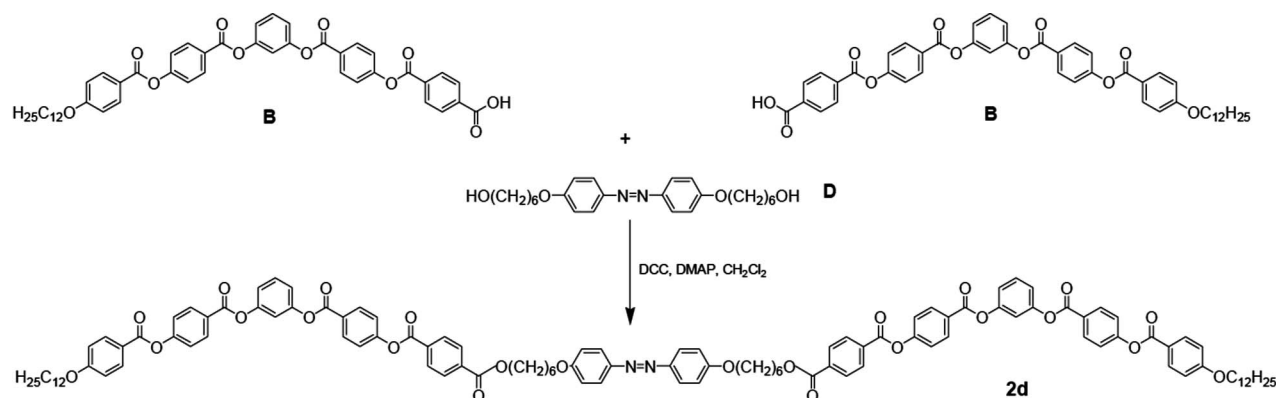
2.1.1.1 Banana-calamitic dimer **1c**

(a) Dodecyloxy-substituted five-ring bent-core benzoic acid **B**.

1.38 g (5.39 mmol) 4-(Benzyloxycarbonyl)benzoic acid were converted in the corresponding acid chloride by means of oxalyl chloride (8 mL of 2 M solution in dichloromethane, 16 mmol) in dichloromethane (50 mL). The crude acid chloride was reacted with



Scheme 2. The reaction pathway for preparing the banana-calamitic dimer, **1c**.



Scheme 3. The final reaction step for preparing the banana-calamitic-banana trimer, **2d**.

(3.13 g, 4.90 mmol) 3-(4-hydroxybenzoyloxy)phenyl 4-(4-dodecyloxybenzoyloxy)benzoate (**A**) in the presence of pyridine (0.5 mL, $d = 0.97$ g/mL, 6.13 mmol) and DMAP (400 mg, 3.28 mmol) in dichloromethane (100 mL). 4.08 g of the crude benzyl ester was immediately used in the de-protection reaction by means of hydrogenolysis with palladium on carbon. The five-ring benzoic acid **B** was purified by crystallisation from chloroform/petroleum ether. The reaction yielded 3.71 g (86% overall) of pure product **B**, white crystals, m.p. 221°C. ^1H NMR (400 MHz, CDCl_3) δ (ppm): 8.23–8.15 (m, 6H, Ar-H), 8.10 (d, $^3J = 8.5$ Hz, 2H, Ar-H), 8.04 (d, $^3J = 8.9$ Hz, 2H, Ar-H), 7.44 (t, $^3J = 8.1$ Hz, 1H, Ar-H), 7.36 (d, $^3J = 8.7$ Hz, 2H, Ar-H), 7.31 (d, $^3J = 8.7$ Hz, 2H, Ar-H), 7.18–7.07 (m, 3H, Ar-H), 6.92 (d, $^3J = 8.9$ Hz, 2H, Ar-H), 3.99 (t, $^3J = 6.5$ Hz, 2H, OCH_2), 1.80–1.68 (m, 2H, OCH_2CH_2), 1.47–1.11 (m, 20H, CH_2), 0.80 (t, $^3J = 6.8$ Hz, 3H, CH_3).

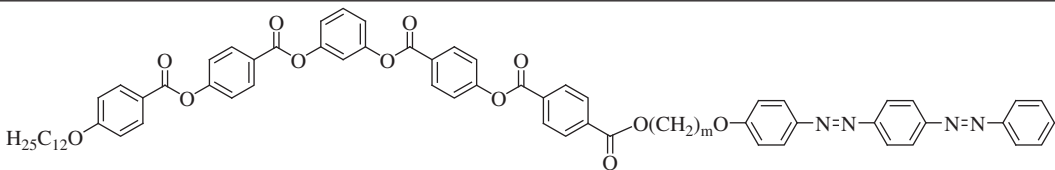
(b) Banana-calamitic dimer **1c**.

0.34 g (0.854 mmol) 4-(6-Hydroxyhexyloxy)bisa-zobenzene **C** and 0.67 g (0.854 mmol) dodecyloxy-substituted five-ring bent-core benzoic acid **B** were dissolved in 50 mL dichloromethane. 0.19 g (0.94 mmol) Dicyclohexylcarbodiimide and a small amount of 4-dimethylaminopyridine as a catalyst was added and the mixture was allowed to stir at room temperature for about 24 h. Dicyclohexylurea was filtered off and the solvent was evaporated. The residue was purified by chromatography on silica gel using chloroform/ethanol (10/0.2) as the eluent. Re-crystallisation from ethyl acetate gave the pure compound **1c**. Yield: 0.77 g, 77.0%, yellow crystals, m.p. 160°C, for the mesophase behaviour see Table 1. Elemental analysis: $\text{C}_{71}\text{H}_{70}\text{N}_4\text{O}_{12}$, $M = 1171.37$ g/mol; C 72.80, H 6.02, N 4.78 (calcd), C 72.77, H 6.23, N 4.69 % (found). ^1H NMR (400 MHz,

CDCl_3) δ (ppm): 8.31–8.22 (m, 6H, Ar-H), 8.17 (d, $J = 8.5$ Hz, 2H, Ar-H), 8.13 (d, $J = 8.9$ Hz, 2H, Ar-H), 8.07–7.96 (m, 4H, Ar-H), 7.93 (d, $J = 8.9$ Hz, 4H, Ar-H), 7.59–7.42 (m, 4H, Ar-H), 7.42–7.30 (m, 4H, Ar-H), 7.22–7.11 (m, 3H, Ar-H), 7.00 (d, $J = 9.01$ Hz, 2H, Ar-H), 6.97 (d, $J = 8.90$ Hz, 2H, Ar-H), 4.40 (t, $J = 6.6$ Hz, 2H, COOCH_2), 4.10–4.01 (m, 4H, OCH_2), 1.91–1.77 (m, 6H, $\text{COOCH}_2\text{CH}_2$, OCH_2CH_2), 1.58–1.18 (m, 22H, CH_2), 0.87 (t, $J = 6.7$ Hz, 3H, CH_3). ^{13}C NMR (101 MHz, CDCl_3) δ (ppm): 165.51, 164.17, 163.96, 163.76, 163.65, 161.89, 155.45, 154.92, 153.89, 153.26, 152.72, 151.39, 135.10, 132.71, 132.37, 131.91, 131.79, 131.20, 130.18, 129.83, 129.73, 129.08, 127.13, 126.60, 125.03, 123.72, 123.39, 122.99, 122.11, 121.91, 119.20, 115.76, 114.79, 114.45, 68.50, 68.24, 65.60, 32.05, 29.79, 29.77, 29.72, 29.69, 29.48, 29.24, 28.77, 26.13, 25.96, 25.93, 22.83, 14.26.

2.1.1.2 Banana-calamitic-banana trimer **2d**.

0.80 g (1.02 mmol) Dodecyloxy-substituted five-ring bent-core benzoic acid **B** and 0.21 g (0.51 mmol) 4,4'-bis(6-hydroxyhexyloxy)azobenzene **D** were dissolved in 50 mL dichloromethane. 0.23 g (1.12 mmol) Dicyclohexylcarbodiimide and a small amount of 4-dimethylaminopyridine as the catalyst were added and the mixture was allowed to stir at room temperature for about 24 h. After separation of the precipitated dicyclohexylurea, the solvent was removed and the residue was purified on silica gel using chloroform/ethanol (10/0.2) as the eluent. The solid material obtained after evaporation the solvent was re-crystallised from ethyl acetate. Yield: 0.62 g, 62.1%, yellow crystals, m.p. 162°C, for the mesophase behaviour see Table 2. Elemental analysis: $\text{C}_{118}\text{H}_{122}\text{N}_2\text{O}_{24}$, $M = 1952.29$ g/mol; C 72.60, H 6.30, N 1.43 (calcd), C 72.41, H 6.47, N 1.17 % (found). ^1H NMR (400 MHz, CDCl_3) δ (ppm): 8.32–8.20

Table 1. Transition temperatures [°C], mesophase type, transition enthalpy values [kJ/mol], layer spacing d [nm], tilt angle τ of the molecules [°] with respect to the layer normal in SmC phases and P_S values of the dimer series **1a–c**^[a]


Comp.	m	Transitions temperatures [°C]		Lattice parameters		P_S nC/cm^2
		ΔH [kJ·mol ⁻¹]		d [nm]	τ [°]	
1a	2	Cr 192 (SmC _a P _A 184) I 86.1	– ^[b]	– ^[c]	– ^[c]	270
1b	4	Cr 176 (SmC _s P _F 161) SmC _a P _A 184 I 45.1	– ^[b] 27.1	6.01 ^[d] 6.10 ^[e]	22.5 ^[d] 20.0 ^[e]	350 ^[d] 470 ^[e]
1c	6	Cr 160 (SmC _s P _F 151) SmC _a P _A 175 I 66.4	0.1 29.0	6.30 ^[d] 6.30 ^[e]	20.0 ^[d] 20.0 ^[e]	590 ^[d] 770 ^[e]

Notes: ^[a] Transition temperatures (°C) and enthalpy values [kJ/mol] were taken from the second DSC heating scans (10 Kmin⁻¹); values in parentheses indicate monotropic mesophases, in this case the transition temperatures and enthalpy values were taken from the first DSC cooling scans and the transition temperatures were checked by polarizing microscopy; ^[b] the transition is not detectable by DSC and the transition temperature is determined by polarizing microscopy; ^[c] could not be determined due to rapid crystallization of the sample; ^[d] values for the SmC_aP_A phase; ^[e] values for the SmC_sP_F phase.

(m, 12H, Ar–H), 8.15 (d, J = 8.3, 4H, Ar–H), 8.13 (d, J = 8.8, 4H, Ar–H), 7.54–7.41 (m, 6H, Ar–H), 7.41–7.31 (m, 8H, Ar–H), 7.22–7.12 (m, 6H, Ar–H), 6.97 (d, J = 8.9 Hz, 4H, Ar–H), 6.92 (d, J = 8.8 Hz, 4H, Ar–H), 4.45 (t, J = 5.9 Hz, 4H, COOCH₂), 4.11–3.99 (m, 8H, OCH₂), 2.09–1.91 (m, 8H, COOCH₂CH₂, OCH₂CH₂), 1.88–1.73 (m, 4H, OCH₂CH₂), 1.51–1.15 (m, 42H, CH₂), 0.87 (t, J = 6.8 Hz, 6H, CH₃). ¹³C NMR (127 MHz, DMSO) δ (ppm): 167.86, 163.56, 163.35, 163.26, 163.22, 163.19, 156.85, 154.89, 154.88, 154.48, 153.39, 141.89, 131.74, 131.21, 131.12, 129.50, 129.33, 129.29, 126.88, 126.23, 125.83, 121.60, 121.46, 120.13, 118.74, 118.68, 115.21, 113.86, 67.75, 54.73, 49.14, 47.69, 33.33, 31.21, 31.18, 30.09, 28.94, 28.92, 28.87, 28.85, 28.65, 28.64, 28.38, 25.45, 25.28, 25.10, 24.70, 24.66, 24.32, 23.97, 21.99, 13.51.

2.2 Methods

The thermal transition behaviour, i.e. the measurement of the temperature dependence of the heat capacity C_p and/or the enthalpy ΔH , was investigated using a Perkin Elmer DSC Pyris 1 differential scanning calorimeter. The texture observations of the liquid crystal films sandwiched between two glass plates were carried out with a Leitz polarising microscope (Laborlux 12 Pol S, Germany). For the electro-optical measurements we used commercial sandwich cells (E.H.C., Japan) with a thickness between 5 and 15 μ m. The majority of the used glass plates exhibit a rubbed polyimide coating for planar surface alignment of the

director. The cells were observed in transmission using a Leica (DMRXP, Germany) polarising microscope equipped with a digital camera Nikon (Coolpix 4500, Japan). The cells were mounted onto a heating stage (Linkam LTS 350, UK, and Mettler, FP82HT und FP90, UK) for temperature control. The magnitude of the spontaneous polarisation was measured by integrating the polarisation reversal current peak obtained by switching the sample with a triangular electric field. X-Ray investigations were performed either on a small droplet of the sample on a glass plate (aligned upon slow cooling at the sample–glass or at the sample–air interface) or on a sample in a glass capillary (aligned using a magnetic field of about 1 T). The droplet-sample was held on a temperature-controlled heating stage, which partially shadows the patterns below the equator. The diffraction patterns were recorded by a 2D detector (HI-STAR, Siemens) using Ni filtered CuK α radiation.

3. Results and discussion

3.1 Mesophase behaviour, phase structures and electro-optical studies

3.1.1 Banana–calamitic dimers **1a–1c** consisting of a five-ring bent-core mesogenic moiety and a calamitic bis(azobenzene) unit

The banana–calamitic dimers **1a–1c** possess a five-ring bent-core moiety, which is connected by flexible spacers to a three-ring calamitic bis-azobenzene unit.

A dodecyloxy chain substitutes one leg of the bent-core molecule. A carboxylic group to the methylene spacer links the second leg, and an etheroxygen atom connects the methylene spacer to the calamitic fragment. That means all dimers **1a–1c** possess an *odd*-numbered spacer with an *even* number of methylene units ($m = 2, 4, 6$). The mesophase behaviour, transition temperatures together with the associated transition enthalpies, lattice parameters and spontaneous polarisation values of the compounds **1a–1c** are collected in Table 1.

All banana–calamitic twin molecules **1a–1c** exhibit smectic phases. Compound **1a** with the shortest spacer ($m = 2$) shows a monotropic smectic phase, while dimers **1b** and **1c** ($m = 4, 6$) form an additional enantiotropic high-temperature smectic phase. The mesomorphic properties of these two homologues that differ due to the two methylene groups are very similar. The clearing temperatures decrease only few degrees with the elongation of the spacer.

Upon cooling dimers **1b** and **1c** from the isotropic liquid state, Schlieren or fan-shaped textures appear, but also fascinating textures with spiral nuclei grow, which coalesce into a variety of textures including ribbon-like and spherulitic textures, focal conics and circular domains, see Figure 1. Some of the textures remind us of those of the B₇ phase family [36, 39, 41, 94, 95].

The presence of well defined circular domains with extinction directions parallel to the position of the crossed polarisers is an argument for the anticlinic organisation of the molecules between adjacent layers in the high-temperature phase (Figure 1(a) and (b)). Furthermore, the observation of a Schlieren texture together with a smooth fan-shaped texture showing irregular stripes across the fans is a strong indication that the high temperature phase could be an anticlinic SmC phase, i.e. a SmC_a phase (Figure 1 and Figure 2(a)).

The transition into the low temperature phase is accompanied by a pronounced change of the textures although the transition enthalpies are very small. The

smooth fan-shaped texture of the high-temperature SmC_a phase is transformed into a more or less non-specific one as shown in Figure 2(a)–(c). In the case of perfectly structured circular domains, a rotation of the extinction crosses can be observed at the phase transition to the low-temperature phase, see Figure 2(d) and (e). The extinction crosses make an angle of $\sim 20^\circ$ with the directions of the crossed polarisers indicating that the low-temperature phase has a synclinic-tilted organisation.

It should be noted that the anticlinic–synclinic transition is accompanied by clear optical effects that are observable in the Schlieren texture. The Schlieren texture becomes strongly fluctuating near the transition of the low-temperature smectic phase (Figure 2(b)) and the number of disclinations increases in the Schlieren texture islands (Figure 2(c)). These are indications of a stepwise transition from the anticlinic to a synclinic organisation of the molecules between adjacent layers. The SmC_a–SmC_s phase transition for compounds **1b** and **1c** ($m = 4, 6$) is characterised by a very small transition enthalpy (about 0.1 kJ/mol). This dimorphism is only rarely observed for non-chiral compounds. It has been reported for hockey stick-shaped mesogens [96–103] and terminally branched mesogens [104–106]. For these compounds the sequence SmC_s–SmC_a was reported on cooling that is, surprisingly, opposite to the sequence of the dimers **1b** and **1c** which is SmC_a–SmC_s with decreasing temperature.

As a representative example, the XRD investigations on the mesophases of dimer **1c** on cooling will be presented in more detail. XRD measurements at 165°C and at 145°C confirmed the presence of the two SmC phases. They show very similar patterns for both phases (Figure 3(a)–(d)). For this compound, the layer spacing derived from the XRD measurements upon cooling is independent of the temperature, including the transition from the high-temperature SmC_a (6.30 nm) to the lower-temperature SmC_s phase (6.30 nm) and indeed until the sample crystallises. An average tilt angle of the molecular long axis with

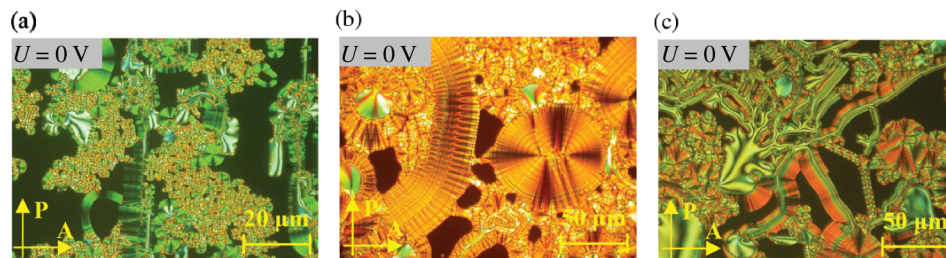


Figure 1. Textures of the high-temperature SmC_aP_A phase of compound **1c** upon cooling the isotropic liquid at 171°C without an electric field in a 5 μm non-coated indium tin oxide (ITO) cell (a) and (c) and in a 6 μm polyimide-coated ITO cell (b).

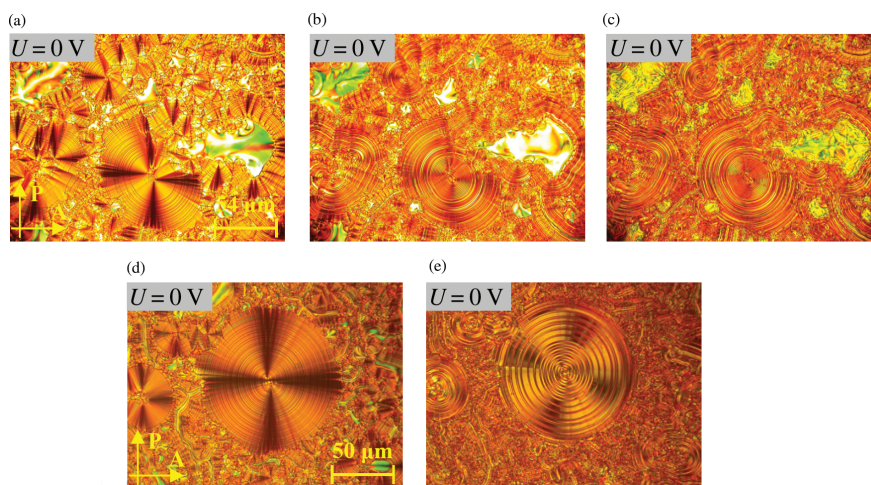


Figure 2. Phase transition SmC_a – SmC_s of compound **1c** upon cooling without an electric field in a 5 μm non-coated ITO cell between crossed polarisers: (a) regions of the high-temperature SmC_a phase showing fan-shaped and Schlieren texture, respectively, at 168°C. (b) Turbulences in the Schlieren texture islands between the two smectic states at 151°C, accompanied by the appearance of additional defects. (c) Disturbed fan-shaped texture and changed Schlieren texture of the low-temperature SmC_s phase at 145°C. (d) and (e) Rotation of the extinction cross at the SmC_a – SmC_s transition, $U = 0$ V in a 6 μm polyimide-coated ITO cell, (d) high-temperature phase at 171°C and (e) in the low-temperature phase at 145°C.

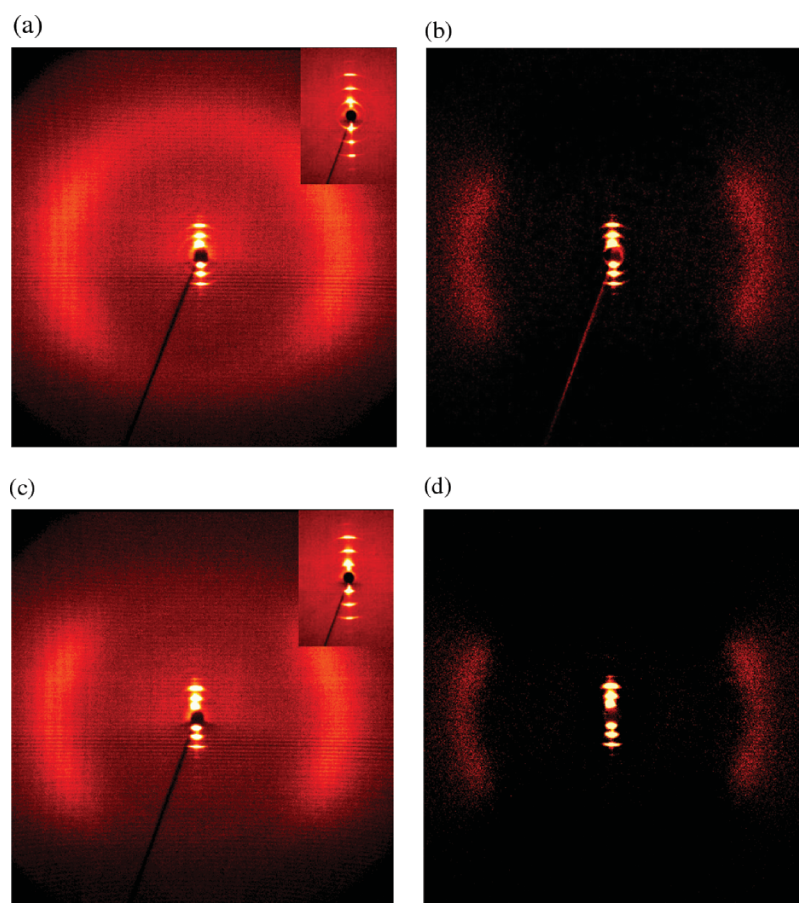


Figure 3. XRD patterns of an aligned sample of compound **1c**: (a) and (b) high-temperature SmC_a phase at 165 °C: (a) original pattern; (b) the same XRD pattern, but the intensity of the isotropic liquid is subtracted. (c) and (d) Low-temperature SmC_s phase at 145°C: (c) original pattern; (d) the same XRD pattern, but the intensity of the isotropic liquid is subtracted; (a) and (c) the insets show the small angle scattering.

respect to the layer normal can be calculated from the position of the maxima for the outer diffuse scattering in both SmC phases ($\tau = 20^\circ$). An effective molecular length L_{eff} may be calculated from these experimental results for both the SmC phases to $L_{\text{eff}} = d/\cos\tau = 6.70$ nm.

The XRD investigations on compound **1b** show a similar behaviour. Interestingly, the layer spacing increases upon cooling, from the high-temperature SmC_a phase (6.01 nm) to the low-temperature SmC_s phase (6.10 nm), accompanied by a tilt angle τ decreasing from 23° in the high-temperature SmC_a phase to 20° in the low-temperature SmC_s phase as derived from the outer diffuse scattering. Because of the fibre-like disorder of the samples, no clear evidence for a transition from an anticlinic to a synclinic organisation of the molecules between adjacent layers can be derived by the XRD investigations.

The electro-optical studies on the high-temperature SmC_a phases of compounds **1b** and **1c** evidenced the occurrence of two separate re-polarisation peaks in each half period of the applied triangular voltage field, which is characteristic of antiferroelectric switching (Figure 4(d)). The calculated values of the spontaneous polarisation vary between 350 (**1b**) and 590 nC/cm² (**1c**). The

application of an electric field (10 V/ μ m) on the high-temperature SmC_a phase leads to the formation of a smoother fan-like texture. In the circular domains, the extinction crosses are aligned along the directions of the crossed polarisers and do not change on applying, on reversal (Figure 4(a) and (c)) or on terminating the applied field (Figure 4(b)). These findings suggest that the antiferroelectric ground state, as well as the switched ferroelectric states, have an anticlinic tilt. This switching corresponds to the transition from an SmC_aP_A state to a SmC_aP_F state. The collective rotation of the molecules around their long axes on reversing the applied field is sketched in Figure 4 below the corresponding texture micrographs.

The low-temperature phase of compounds **1b** and **1c** also shows an electro-optical response. The SmC_s phase presents one well-defined re-polarisation peak per half period of the applied triangular voltage field, which allows a designation as SmC_sP_F phase (Figure 5(d)). To prevent an artefact, a modified triangular-wave field was also applied using non-coated ITO cells and different cell thickness or glass coatings (5, 6, 10 or 15 μ m). Also in these cases, only one peak per half period of the applied field could be observed. The calculated spontaneous polarisation

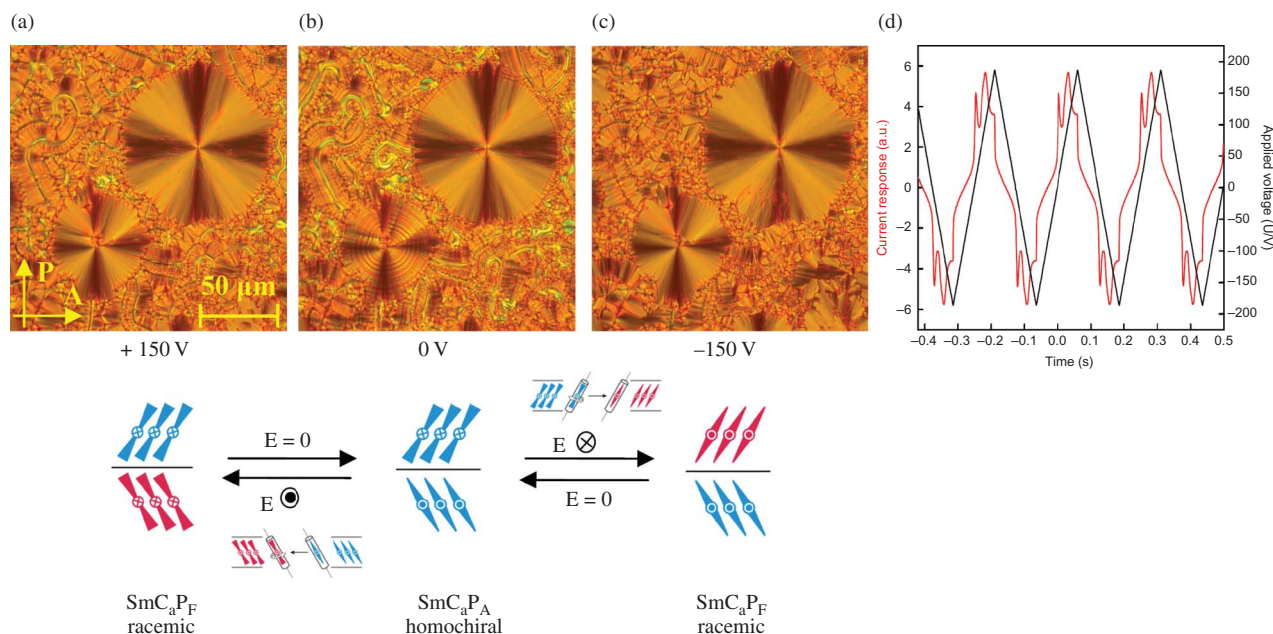


Figure 4. Electro-optical investigations on the SmC_aP_A phase of compound **1c** at 165°C observed between crossed polarisers in a 5 μ m non-coated ITO cell: (a) and (c) $U = \pm 150$ V. (b) $U = 0$ V. (d) Antiferroelectric switching current response obtained by applying a triangular-wave voltage ($U = 373$ V_{pp}, $f = 4$ Hz, $R = 5$ k Ω , spontaneous polarisation = 590 nC/cm²). Below the textures the corresponding switching process of the molecules in the layers in the FE state (a) and (c) and in the AF ground state (b) is shown. In the schematic model, only the bent-core parts of the dimers are shown because the calamitic moieties are not of importance for the electro-optical behaviour under discussion. The colours blue and red indicate the different chirality sense.

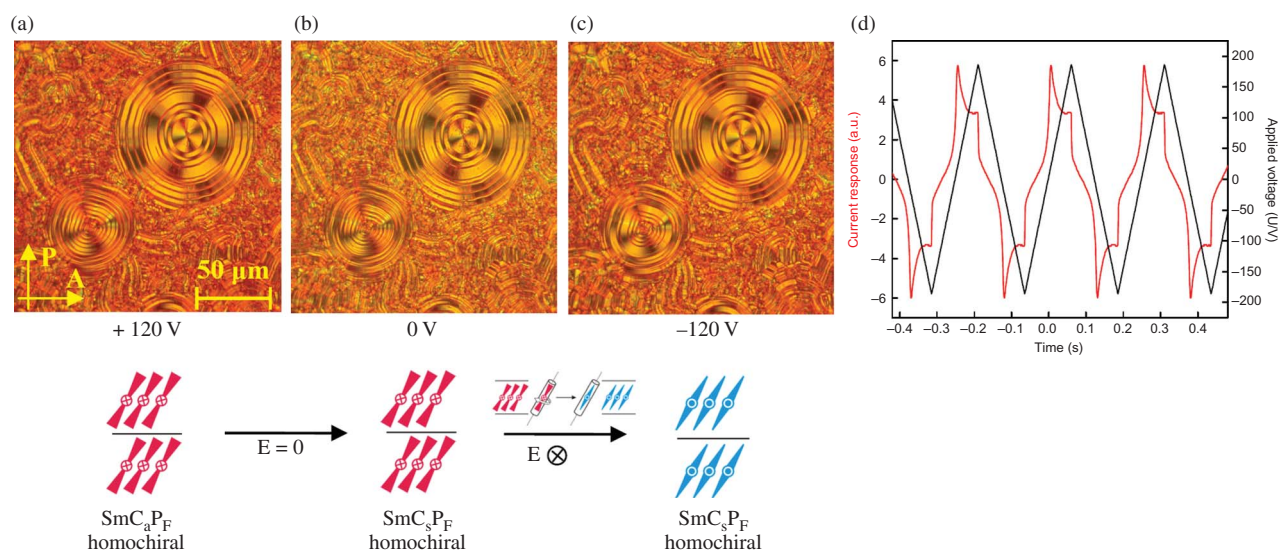


Figure 5. Electro-optical investigations on the SmC_sP_F phase of compound **1c** under a d.c. electric field at 145°C observed between crossed polarisers in a $5\ \mu\text{m}$ non-coated ITO cell: (a) and (c) $U = \pm 120\ \text{V}$. (b) $U = 0\ \text{V}$. (a)–(c) Models of the organisation of the molecules in both ferroelectric states in the bistable switching process. (d) FE switching current response obtained by applying a simple triangular-wave voltage ($5\ \mu\text{m}$ non-coated ITO cell, $U = 372\ \text{V}_{\text{pp}}$, $f = 4\ \text{Hz}$, $R = 5\ \text{k}\Omega$, $T = 145^\circ\text{C}$, spontaneous polarisation $= 770\ \text{nC}/\text{cm}^2$).

values amount to 470 (**1b**) and to $770\ \text{nC}/\text{cm}^2$ (**1c**). The extinction directions of the circular domains make an angle of $\sim 20^\circ$ with the directions of the crossed polarisers indicating that this SmC phase has a tilted organisation (Figure 5(a)–(c)). If the first ferroelectric ground state (Figure 5) is switched to the second ferroelectric state or *vice versa*, the extinction directions do not change and only the birefringence slightly varies (Figure 5(c)). Furthermore, this effect is independent of the polarity of the applied field. Hence, the ferroelectric ground state as well as the switched ferroelectric states has a synclitic tilt and the switching corresponds to the transition between two SmC_sP_F states. The chirality of the layers switches by a collective rotation of molecules around their long axes on reversing the applied field.

The early crystallisation of the monotropic smectic phase of dimer **1a** prevents a structural characterisation by XRD studies. However, the electro-optical experiments were possible and they evidenced a SmC_aP_A phase, which has similar properties to those found for the SmC_aP_A phases of the homologues **1b** and **1c**.

The dimers **1b** and **1c** and several hockey stick-shaped compounds exhibit the rare synclitic–anticlinic SmC phase transition [96–103]. For both types of materials, this phase transition is characterised by strong turbulences in the textures and by low transition enthalpies. Therefore, a comparison of

the electro-optical behaviour is also of interest. The situation is clear for the dimers studied here as evidenced before: both SmC phases are polar phases showing current response curves typical for SmCP phases. The situation is different for the SmC phases formed by hockey stick-shaped compounds: neither the polar character nor the electro-optical behaviour is clear. Stannarius et al. reported a low, but clearly measurable spontaneous polarisation for the high-temperature SmC phase of the hockey-stick mesogens in free-standing films [99]. In contrast, measurements by means of null transmission ellipsometry and depolarised reflected light microscopy on very thin films of definite number of layers between two and ten using the same material by Huang et al. [101, 107] have not given evidence for polar properties of both SmC phases. Chakraborty et al. reported for a series of hockey stick-shaped mesogens a current response with two peaks for the synclitic and the anticlinic SmC phases, which however do not completely disappear upon heating into the isotropic phase [108]. Yu et al. observed a similar behaviour for other hockey-stick compounds [96, 97]. The effect could be explained by a field-induced switching corresponding to a Fredericksz transition or by latently polar properties of the SmC phases [109]. In summary, the electro-optical behaviour of synclitic and anticlinic SmC phases formed by hockey stick-shaped mesogens is not really conclusive.

3.1.2 Banana–calamitic–banana trimers containing an azobenzene bridge between two bent-core mesogenic moieties, compounds **2a–2d**

Compounds **2a–2d** represent a novel type of trimers that have not been reported until now. They consist of two bent-core mesogenic units and one calamitic unit. In compounds **2a–2d**, an azobenzene moiety serves as bridge between two five-ring bent-core moieties. The three mesogenic units are linked to the alkylene spacers of different length ($m = 2, 4, 5, 6$) by the groups –COO– and –O–. The chemical structure of the trimers is a symmetric one, the dodecyloxy chains are attached to both terminal positions. The mesophase behaviour is given in Table 2.

For compounds **2a** and **2b** with spacer lengths of $m = 2$ and 4, the LC behaviour could not be observed, whereas the homologous members with $m = 5$ and 6 exhibit smectic phases.

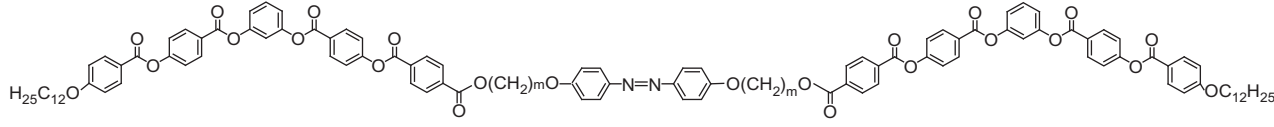
Compound **2c** ($m = 5$) forms two mesophases, which could be identified as smectic modifications. The molecular long axes are tilted with respect to the layer normal as proved by their characteristic textures, i.e. Schlieren, high- and low-birefringent fan-shaped textures and regions with circular domains, where the extinction crosses are aligned or inclined with respect to the position of the crossed polarisers. It was impossible to obtain homeotropic textures by shearing or by surface treatment, which excluded the existence of smectic phases with orthogonally directed molecules. The corresponding phase transition is characterised by a small transition enthalpy (about 0.3 kJ/mol). Fast crystallisation prevented XRD measurements and electro-optical studies. Therefore, both the metastable mesophases of compound **2c** were assigned as SmC_x

and SmC'_x phases, as a complete characterisation of these phases was not possible.

Trimer **2d**, with the longest spacers ($m = 6$), exhibits one monotropic smectic phase. The growth of this phase could give a hint for a columnar or an undulated smectic phase, i.e. upon cooling from the isotropic liquid state a dendritic growth of the texture appears (Figure 6(a)). Additionally, a birefringent texture containing sharp lines and leaf-like patterns, mosaic-like regions and low-birefringent focal conic regions could be observed (Figure 6(a) and (b)). Numerous regions with circular domains with the direction of the extinction crosses parallel to the position of the crossed polarisers suggest an anticlinic organisation of the molecules between adjacent layers. However, the XRD patterns show only layer reflections with $d=6.21$ nm, confirming a smectic phase (Figure 6(c)). The wide-angle pattern of a partially aligned sample indicates a tilted smectic mesophase.

In the electro-optical studies, an antiferroelectric polar switching could be observed. Two current peaks per half-period of a triangular voltage could be recorded during the switching process indicating an SmC_aP_A phase with an antiferroelectric ground state (spontaneous polarisation = 270 nC/cm², see Figure 7(c)). If an electric field of 15 V/μm is applied to this phase the texture becomes *non-specific* and the birefringence slightly increases. The texture of the switched states is independent of the polarity of the field and nearly the same as in the field-off state (Figure 7(a) and (b)). This confirms that the switching between the antiferroelectric ground state and the switched ferroelectric states preferably takes place by a collective rotation of the molecules around their long

Table 2. Transition temperatures^[a] [°C], mesophase type and transition enthalpy values [kJ/mol] of series **2**



Comp.	m	Transitions temperatures [°C] ΔH [kJ·mol ⁻¹]
2a	2	Cr 216 I 111.7
2b	4	Cr 185 I 135.9
2c	5	Cr 187 (SmC'_x 162 SmC_x 176) I 132.4 0.3 33.4
2d	6	Cr 162 (SmC_aP_A 157) I 113.1 43.1

Notes: ^[a] Transition temperatures (°C) and enthalpy values [kJ/mol] were taken from the second DSC heating scans (10 Kmin⁻¹); values in parentheses indicate monotropic mesophases, in this case the transition temperatures and enthalpy values were taken from the first DSC cooling scans and the transition temperatures were checked by polarizing microscopy.

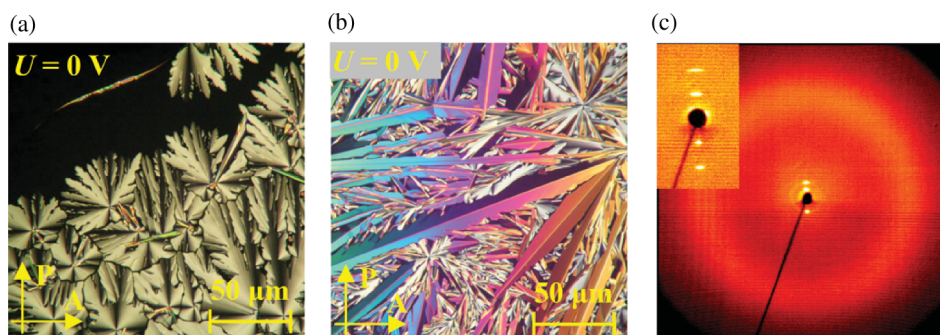


Figure 6. SmCaPA phase of compound **2d**: (a) dendritic growing of the texture on cooling from the isotropic liquid at $U = 0$ V at 157°C and (b) another region showing banana-leaf texture at 150°C . (c) XRD patterns of a partially surface-aligned sample at 148°C ; the inset shows the small angle region.

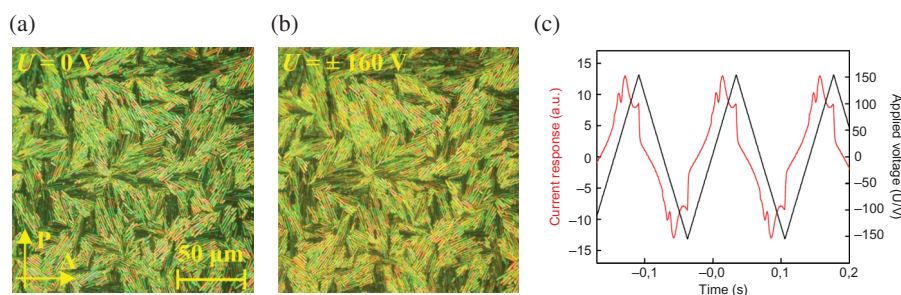


Figure 7. SmCaPA phase of dimer **2d** at 150°C observed between crossed polarisers in a $5\text{ }\mu\text{m}$ non-coated ITO cell: (a) and (b) under a d.c. electric field (a) $U = 0$ V. (b) $U = \pm 160$ V. (c) AF switching current response obtained by applying a triangular-wave voltage ($U = 320\text{ V}_{\text{pp}}$, $f = 4\text{ Hz}$, $R = 5\text{ k}\Omega$, spontaneous polarisation = 270 nC/cm^2).

axes in analogy to the diagram of the switching process as shown in Figure 4.

3.2 Photochemical investigations

3.2.1 Techniques

The photochemical properties were studied using a special instrument equipped with a DRSh-250 ultra-high pressure mercury lamp with 365 nm interference filter and KLM-473/h-150 diode laser (473 nm). To prevent heating of the samples due to infrared (IR) irradiation of the lamp, a water filter was applied. To obtain a plane-parallel light beam, a quartz lens was used. The intensity of light was equal to 3.0 mW/cm^2 (365 nm, non-polarised), 0.9 mW/cm^2 (365 nm, polarised), and $\sim 2\text{ W/cm}^2$ for the laser, as measured by a LaserMate-Q (Coherent) intensity meter. Spectral measurements were performed using a Unicam UV-500 spectrophotometer.

The orientational order was studied using polarised UV/visible spectroscopy, because the transition moment of the *E*-isomer of the azobenzene moiety is directed along the long axis of this group. For this purpose, the angular dependence of the polarised light absorbance was measured using a

photodiode array UV/visible spectrometer (J & M) with a step-width of 10° .

The dichroism values were calculated from the spectra using Equation (1):

$$D = (A_{\parallel} - A_{\perp}) / (A_{\parallel} + A_{\perp}) \quad (1)$$

where A_{\parallel} is the polarised light absorbance at the preferred direction of the chromophore orientation and A_{\perp} is the absorbance perpendicular to this direction. In all cases the polarisation plane of the incident light was 90° with respect to the main axis of the chromophore. A number of films were prepared by the spin-coating method from chloroform solutions of the substances ($\sim 30\text{ mg/mL}$). The thickness of the films was estimated by AFM method (Ntegra, NT-MDT, Russia) and was in the range of $100\text{--}150\text{ }\mu\text{m}$.

3.2.2 Results of the photochemical studies

One member of each series was selected for the photochemical studies. Firstly, the photochemical behaviour of the substances **1c** and **2d** in dilute solutions and films was observed. The spectral changes under UV

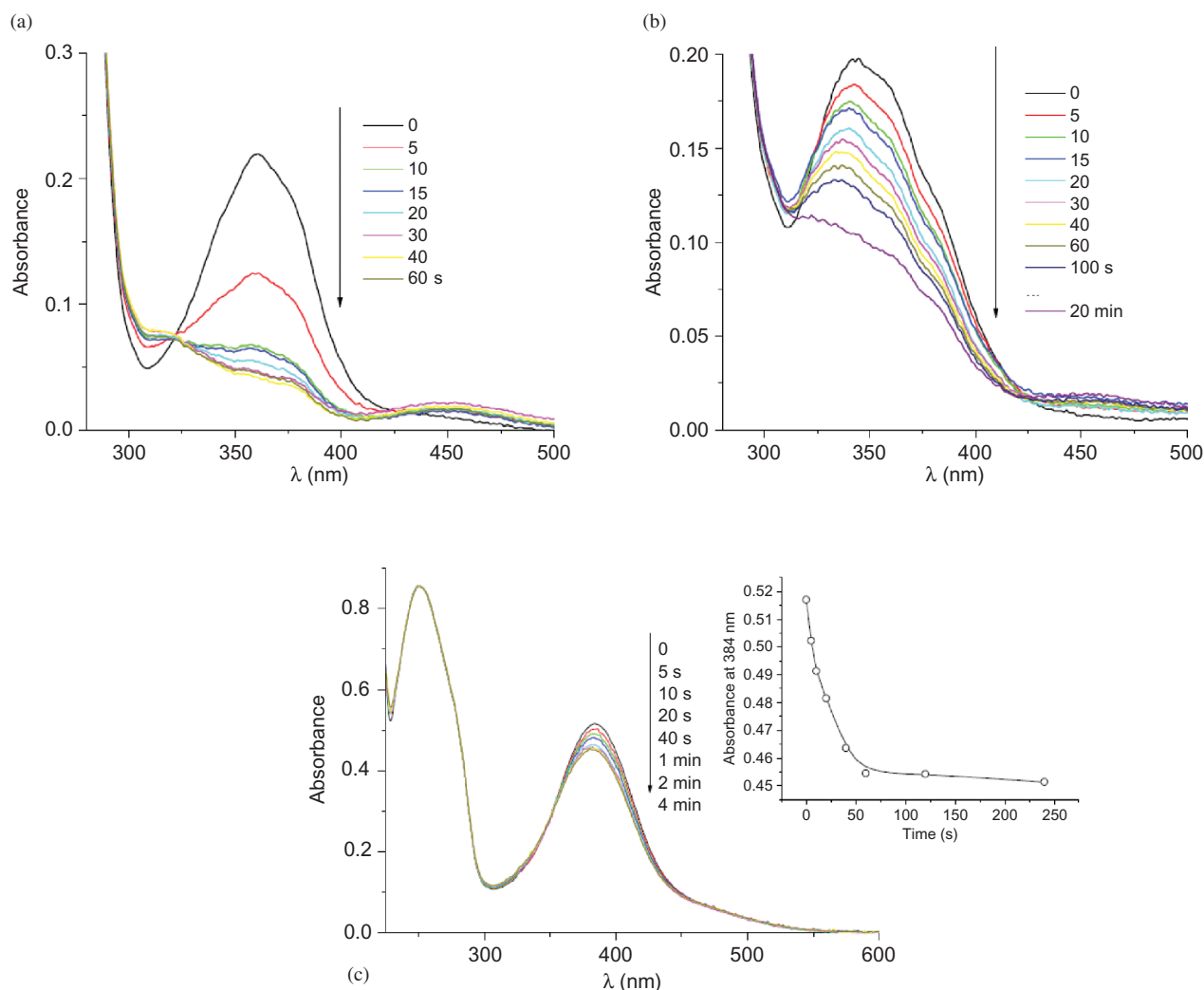


Figure 8. Spectral changes under UV irradiation (365 nm) of (a) the solution of compound **2d** in dichloromethane (1.6×10^{-2} mg/mL). (b) Film of compound **2d**. (c) Solution of **1c** in dichloromethane (1.2×10^{-2} mg/mL). The inset in (c) shows the corresponding kinetics at 384 nm.

irradiation of a **2d** solution are shown in Figure 8(a) and those of the thin spin-coated film are shown in Figure 8(b). As clearly seen from the figures, in both cases the irradiation results in a decrease in the absorbance corresponding to the π - π^* electronic transition of the azobenzene chromophores. Such changes are associated with the *E*-*Z* isomerisation process of the azobenzene moieties. It is noteworthy that spectral changes in case of the dilute solution are more pronounced than in case of the film. Moreover, the time for reaching the photostationary state is strongly different: ~ 1 min for the solution and ~ 20 min for the film. This difference can be explained by the steric hindrance, which suppresses the isomerisation processes and the transition from the rod-like *E*-isomer to the non-linear *Z*-isomer of the azobenzene molecules in solid films of compound

2d. Similar effects are well known in the literature for amorphous and LC azobenzene-containing polymers [110–112].

In contrast to the azobenzene-containing trimer **2d**, the irradiation of a solution of the bis-azobenzene containing dimer **1c** induces only a small decrease in absorbance (Figure 8(c)) and, moreover, there are no spectral changes in the films. Irradiation with light of other wavelength (365, 405, 436 nm) has shown the same tendency. The absence of the *E*-*Z* isomerisation is probably related to the electronic structure of the chromophores having two conjugated azobenzene fragments.

The spin-coating method allowed for the preparation of thin (~ 100 – 200 nm) homogeneous films for compounds **2d** and **1c**. Surprisingly, despite the high melting temperature, these films do not show any

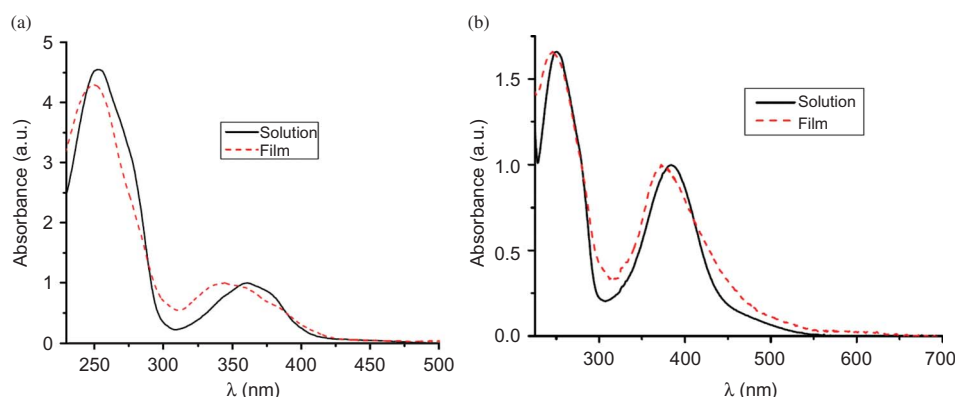


Figure 9. Normalised absorbance spectra of the compounds **2d** (a) and **1c** (b) in dichloromethane solutions and in spin-coated films.

light scattering or birefringence at room temperature, which may be associated with an amorphous disordered state or a crystalline phase consisting of very small crystallites. Figure 9 shows the difference in the absorbance spectra of dichloromethane solutions and spin-coated films. For both compounds a small shift of the absorbance maximum to shorter wavelengths was found. This effect is probably associated with an H-aggregation of the azobenzene chromophores, i.e. with a tendency to their parallel packing [113].

Let us consider the most important part of our work concerning the study of the photo-orientation processes in the thin spin-coated films. In the case of the mono-azobenzene-substituted trimer **2d** irradiation with both, UV and visible polarised light, results in a pronounced anisotropy of absorbance (Figure 10 and Figure 11). The appearance of dichroism indicates a photo-induced orientation of the chromophores in a direction perpendicular to the polarisation plane of the incident light. The polar diagram in Figure 10(c) clearly gives evidence of the good uniaxial orientation. Interestingly, after light action, the absorbance maximum is shifted to shorter wavelengths (Figure 10(a) and (b)). This can be explained by an improvement of aggregation of the chromophores during the photo-orientation process.

The maximum values of dichroism are lower in case of polarised UV light than for blue light due to a noticeable concentration of the *Z*-isomer that to some extent destroys the orientation because of its low anisotropy.

For the bis-azobenzene derivative **1c**, polarised UV light did not induce any anisotropy, whereas irradiation by blue laser allowed one to achieve a similar degree of photo-induced orientation (Figure 12 and Figure 13). During irradiation, the absorbance of light polarised parallel to the preferred orientation increases, whereas the perpendicular one decreases

(Figure 13(a)). At the same time, the averaged non-polarised absorbance remains almost unchanged during irradiation. This allows us to conclude, that no *E*–*Z* isomerisation takes place in the films of this substance, and most probably the mechanism of photo-orientation for compound **1c** is a rotational diffusion associated with cycles of excitation–rotation [114].

It is worth noting that the values of the photo-induced dichroism are almost equal for both substances (~ 0.3). This value of dichroism is more than two times lower than the maximum value obtained for azobenzene-containing side-chain polymers (~ 0.7) [15], but, nevertheless, is much higher than that reported before for glassy amorphous low-molar mass compounds [31–33]. The relatively low values of the dichroism in comparison with the azobenzene-containing polymers can be explained by the presence of bent-shaped fragments that decrease the uniaxial orientation and anisotropy.

We have examined the thermal and temporal stability of the photo-induced order in oriented films. For both compounds, the orientation is very stable at room temperature, at least for several weeks, but as seen in Figure 14, this decreases to zero under heating. Surprisingly, for **2d**, the decrease of the dichroism value starts at about 20°C below the melting temperature (Figure 14(a)) (below 140°C, whereas m.p. is 162°C). Probably the mobility of the molecules at high temperatures, even in the crystalline phase, is strong enough for their reorientation. The heating of this substance above the melting point results in a dewetting process and the formation of small droplets, which crystallise at temperatures below the melting point.

For compound **1c** the orientation is stable up to the melting process (Figure 14(b)). Moreover, the mesophase that has a higher viscosity stabilises the

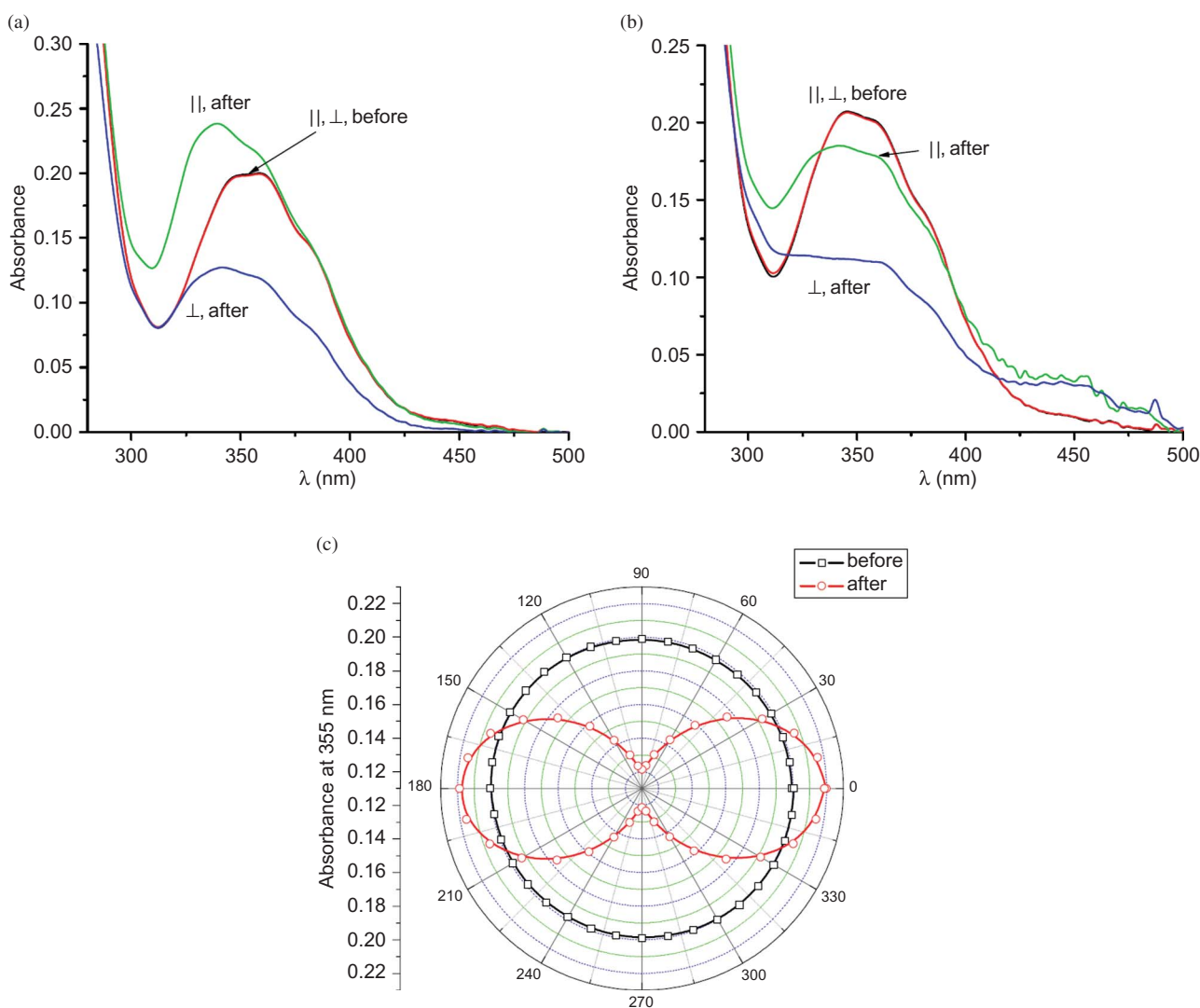


Figure 10. Polarised absorbance spectra of **2d** film (a) before and after 80 min of irradiation with polarised blue light (473 nm). (b) Before and after 100 min of irradiation with UV light. (c) Polar plot of absorbance before and after blue light action.

film and after cooling the sample shows a polycrystalline texture without any preferred orientation. It is important to note that irradiation of the polycrystalline sample by blue polarised light does not lead to any photo-induced anisotropy, i.e. the crystalline order prevents any rotational molecular diffusion.

4. Conclusions

Beside rod-like and discotic mesogens, bent-core mesogens represent the third basic group of low-molecular mass liquid crystals. Members of the different groups form different types of mesophases, such as calamitic, columnar and banana phases, which exhibit only a limited miscibility with each other. If mesogens belonging to different groups are covalently connected

to each other, the existence and the type of mesophases of the new materials cannot be foreseen. In the case of trimers consisting of two discotic and one bent-core mesogenic moieties, for example, the LC properties are lost. The linking of calamitic and banana-shaped mesogens is a more successful concept as reviewed in the introduction and proved in this paper.

The linking of a bent-core mesogen with a calamitic bis(azobenzene) moiety by means of a flexible spacer results in dimers **1a–1c** that exhibit polar smectic phases. Two of the homologues (**1b** and **1c**) bearing a spacer with lengths $m = 4$ and 6 show an exciting behaviour. Both exhibit two SmC phases; these are synclinic and anticlinic SmC phases and only differ in the direction of tilt in the adjacent layers. The SmC_a–SmC_s phase transitions have been rarely found

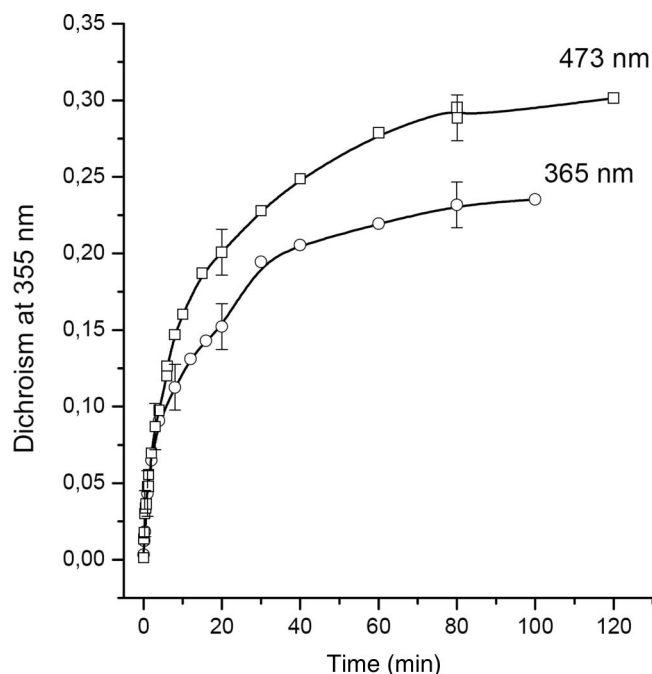


Figure 11. Kinetics of growth of dichroism in films of compound **2d** under irradiation with blue light, 473 nm and UV-light, 365 nm.

for non-chiral compounds. They have been reported so far only for hockey stick-shaped mesogens and for terminally branched mesogens. Remarkably, the new banana-calamitic dimers **1b** and **1c** form the SmC_a and SmC_s phases in the inverse sequence compared with the other non-chiral compounds. For the latter the sequence, the SmC_s – SmC_a transition was found with decreasing temperature. In contrast, the SmC_aP_A phase for the dimers **1b** and **1c** is observed at higher

temperatures and the transition to SmC_sP_F upon cooling. For the banana-calamitic-banana trimers **2**, smectic phases could only be detected for the homologues with a spacer length of $m = 5$ and 6. The smectic phase of trimer **2d** having two spacers with $m = 6$ could be assigned to the SmC_aP_A phase by means of XRD and electro-optic measurements.

The photochemical properties of the two novel bent-shaped substances having photoactive azobenzene fragments were studied in solution and film form. It was found that the irradiation by polarised light induces photo-orientation in the thin amorphous films obtained by spin coating. The kinetics and mechanism of the photo-orientation process were studied and it was shown that the photo-induced order is quite stable at temperatures below the melting transition.

The continuation of the experimental work could serve several different objectives. As mentioned above, nematic phases formed by the bent-core mesogens are of special interest. To find such nematic phases, the chemical structure of the molecules under study should be changed. In principal, we could shorten the terminal alkyloxy chains, decouple the mesogens by longer spacer, or change the ratio between bent-core and calamitic moieties. Therefore, for calamitic-banana-calamitic trimers the existence of nematic phases is more probable. For the photochemical properties, the increase of the photo-orientational effect would be of interest. A further elongation of the oligomeric molecules could achieve this. Furthermore, the influence of stiffness and flexibility on the photo-orientation is unknown for the azobenzene containing materials under discussion.

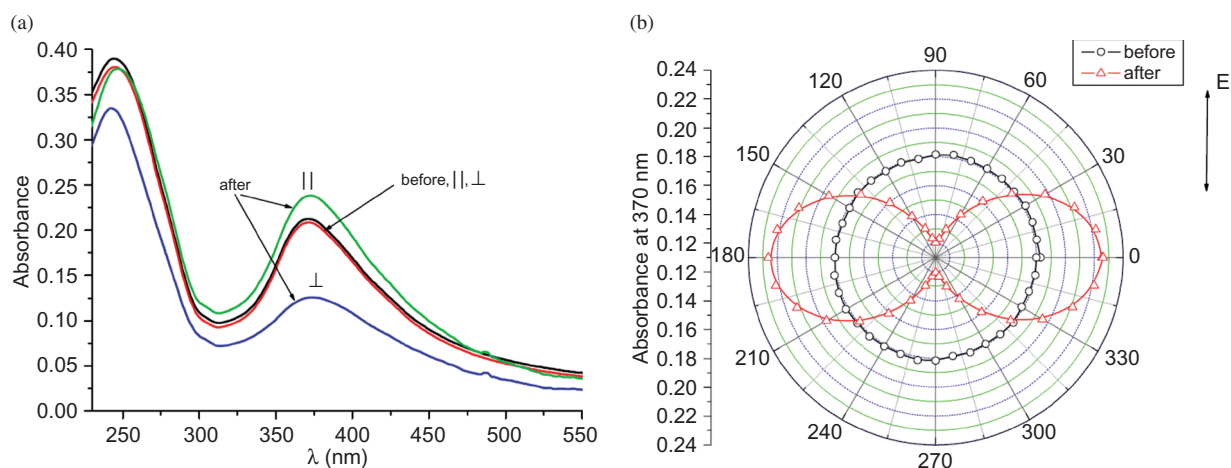


Figure 12. Polarised absorbance spectra of a spin-coated film of **1c** before and after irradiation by blue light (473 nm, 60 min) (a) and the corresponding polar plot of polarised absorbance before and after irradiation (b).

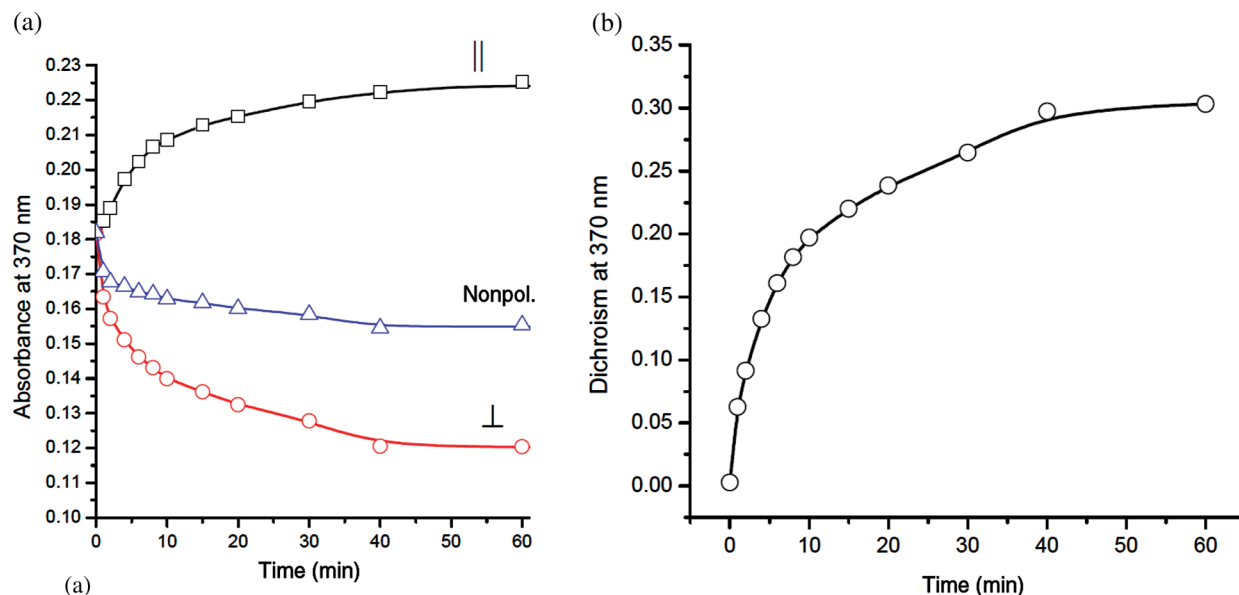


Figure 13. Kinetics of the changes in the polarised absorbance in a film of compound **1c** measured parallel and perpendicular to orientational direction (a) and kinetics of the growth of dichroism (b).

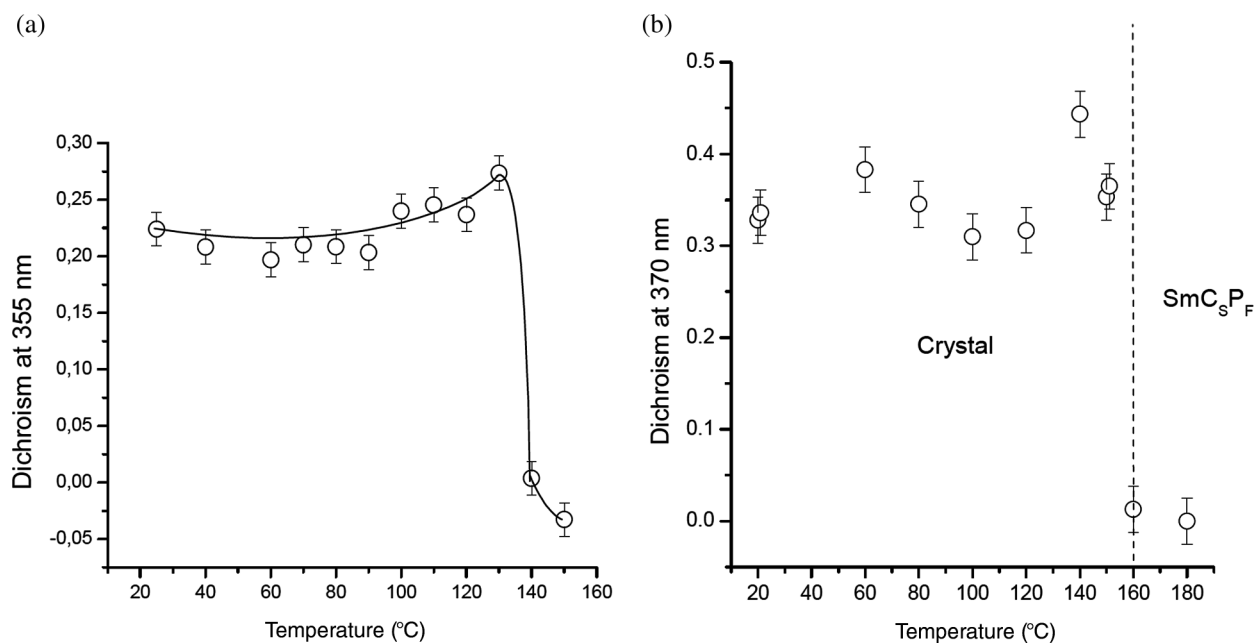


Figure 14. Thermal stability of the photo-induced dichroism in films prepared from compounds **2d** (a) and **1c** (b). The irradiated films were heated up from room temperature.

Acknowledgements

This research was supported by the Russian Foundation of Fundamental Research (11-03-01046a and 11-03-12054-OFI-M), the European Program COST-D35, and the Deutsche Forschungsgemeinschaft. The authors are very thankful to Dr K. Mochalov for the AFM measurements to determine the thickness of the spin-coated films.

References

- [1] Dürr, H.; Bouas-Laurent, H. ed.; *Photochromism: Molecules and Systems*, Elsevier: Amsterdam 2003.
- [2] Shibaev, V.; Bobrovsky, A.; Boiko, N. *Prog. Polym. Sci.* **2003**, 28, 729–836.
- [3] Shibaev, V.P. *Polymers as Electrooptical and Photooptical Active Media*, Springer: Berlin, 1996.

- [4] Ikeda, T. *J. Mater. Chem.* **2003**, *13*, 2037–2057.
- [5] Matharu, A.S.; Jeeva, S.; Ramanujam, P.S. *Chem. Soc. Rev.* **2007**, *36*, 1868–1880.
- [6] Zhao, Y.; Ikeda, T. *Smart Light-Responsive Materials: Azobenzene-Containing Polymers and Liquid Crystals*, Wiley & Sons Inc: Hoboken, N.J., 2009.
- [7] Chigrinov, V.; Kozenkov, V.; Kwok, H.-S. *Photoalignment of Liquid Crystals Materials: Physics and Application*, Wiley-SID series in Display Technology, John Wiley & Sons, Ltd., 2008.
- [8] Weigert, F. *Verhandlungen der Deutschen Physikalischen Gesellschaft* **1919**, *21*, 479–491.
- [9] Buffeteau, T.; Lagugné-Labarthe, F.; Sourisseau, C.; Kostromine, S.; Bieringer, T. *Macromolecules* **2004**, *37*, 2880–2889.
- [10] Cojocariu, C.; Rochon, P. *Pure Appl. Chem.* **2004**, *76*, 1479–1497.
- [11] Dall'Agnol, F.F.; Oliveira, Jr., O.N.; Giacometti, J.A. *Macromolecules* **2006**, *39*, 4914–4919.
- [12] Priimagi, A.; Vapaavuori, J.; Rodriguez, F.J.; Faul, C.F.J.; Heino, M.T.; Ikkala, O.; Kauranen, M.; Kaivola, M. *Chem. Mater.* **2008**, *20*, 6358–6363.
- [13] Koshiha, Y.; Yamamoto, M.; Kinashi, K.; Misaki, M.; Ishida, K.; Oguchi, Y.; Ueda, Y. *Thin Solid Films* **2009**, *518*, 805–809.
- [14] Tejedor, R.M.; Serrano, J.-L.; Oriol, L. *Eur. Polym. J.* **2009**, *45*, 2564–2571.
- [15] Fernández, R.; Mondragon, I.; Galante, M.J.; Oyanguren, P.A. *Eur. Polym. J.* **2009**, *45*, 788–794.
- [16] Gimeno, S.; Forcén, P.; Oriol, L.; Piñol, M.; Sánchez, C.; Rodríguez, F.J.; Alcalá, R.; Jankova, K.; Hvilsted, S. *Eur. Polym. J.* **2009**, *45*, 262–271.
- [17] Uekusa, T.; Nagano, S.; Seki, T. *Macromolecules* **2009**, *42*, 312–318.
- [18] Wolfer, P.; Audorff, H.; Kreger, K.; Kador, L.; Schmidt, H.-W.; Stingelina, N.; Smith, P. *J. Mater. Chem.* **2011**, *21*, 4339–4345.
- [19] Stumpe, J.; Lasker, L.; Fischer, Th.; Kostromin, S.; Ivanov, S.; Shibaev, V.; Ruhmann, D. *Mol. Cryst. Liq. Cryst.* **1994**, *253*, 1–10.
- [20] Brown, D.; Natansohn, A.; Rochon, P. *Macromolecules* **1995**, *28*, 6116–6123.
- [21] Ramanujam, P.; Holme, N.; Hvilsted, S. *Appl. Phys. Lett.* **1996**, *68*, 1329–1331.
- [22] Natansohn, A.; Rochon, P.; Meng, X.; Barret, C.; Buffeteau, T.; Bonenfant, S.; Pezolet, M. *Macromolecules* **1998**, *31*, 1155–1161.
- [23] Geue, Th.; Ziegler, A.; Stumpe, J. *Macromolecules* **1997**, *30*, 5729–5738.
- [24] Hvilsted, S.; Andruzzi, F.; Kulinna, Ch.; Siesler, H.; Ramanujam, P. *Macromolecules* **1995**, *28*, 2172–2183.
- [25] Buffeteau, Th.; Pezolet, M. *Macromolecules* **1998**, *31*, 2631–2635.
- [26] Blinov, L. M.; Barberi, R.; Cipparrone, G.; Iovane, M.; Checco, A.; Lazarev, V. V.; Palto, S. P. *Liq. Cryst.* **1999**, *26*, 427–436.
- [27] Yaroshchuk, O.; Agra, D. M. G.; Zakrevskyy, Yu.; Chien, L.-C.; Lindau, J.; Kumar, S. *Liq. Cryst.* **2001**, *28*, 703–707.
- [28] Wu, Y.; Mamiya, J.; Kanazawa, A.; Shiono, T.; Ikeda, T.; Zhang, Q. *Macromolecules* **1999**, *32*, 8829–8835.
- [29] Bobrovsky, A.; Boiko, N.; Shibaev, V.; Stumpe, J. *Liq. Cryst.* **2002**, *29*, 1469–1476.
- [30] Meier, J. G.; Ruhmann, R.; Stumpe, J. *Macromolecules* **2000**, *33*, 843–850.
- [31] Tanino, T.; Takahashi, T.; Nakano, H.; Shirota, Y. *Mol. Cryst. Liq. Cryst.* **2005**, *430*, 193–198.
- [32] Shirota, Y.; Moriwaki, K.; Yoshikawa, S.; Ujike, T.; Nakano, H. *J. Mater. Chem.* **1998**, *8*, 2579–2581.
- [33] Grebenkin, S.Yu.; Bol'shakov, B.V. *J. Photochem. Photobiol. A: Chem.* **2006**, *184*, 155–162.
- [34] Niori, T.; Sekine, T.; Watanabe, J.; Takezoe, H. *J. Mater. Chem.* **1996**, *6*, 1231–1233.
- [35] Link, D.R.; Natale, G.; Shao, R.; MacLennan, J.E.; Clark, N.A.; Korblova, E.; Walba, D.M. *Science* **1997**, *278*, 1924–1927.
- [36] Pelzl, G.; Diele, S.; Weissflog, W. *Adv. Mater.* **1999**, *11*, 707–724.
- [37] Walba, D.M.; Korblova, E.; Shao, R.; MacLennan, J.E.; Link, D.R.; Glaser, M.A.; Clark, N.A. *Science* **2000**, *288*, 2181–2184.
- [38] Jakli, A.; Krüerke, D.; Sawade, H.; Heppke, G. *Phys. Rev. Lett.* **2001**, *86*, 5715–5718.
- [39] Amaranatha Reddy, R.; Tschierske, C. *J. Mater. Chem.* **2006**, *16*, 907–961.
- [40] Hird, M. *Liq. Cryst. Today* **2005**, *14*, 9–21.
- [41] Takezoe, H.; Takanishi, Y. *Jpn. J. Appl. Phys.* **2006**, *45*, 597–625.
- [42] Prasad, V. *Liq. Cryst.* **2001**, *28*, 145–150.
- [43] Prasad, V. *Liq. Cryst.* **2001**, *28*, 643–646.
- [44] Prasad, V. *Mol. Cryst. Liq. Cryst.* **2001**, *363*, 167–179.
- [45] Prasad, V.; Jakli, A. *Liq. Cryst.* **2004**, *31*, 473–479.
- [46] Prasad, V.; Kang, S.-W.; Qi, X.; Kumar, S. *J. Mater. Chem.* **2004**, *14*, 1495–1502.
- [47] Jakli, A.; Prasad, V.; Shankar Rao, D.S.; Liao, G.; Jánosy, I. *Phys. Rev. E* **2005**, *71*, 021709–1–021709-6.
- [48] Folcia, C.L.; Alonso, I.; Ortega, J.; Etxebarria, J.; Pintre, I.; Ros, M.B. *Chem. Mater.* **2006**, *18*, 4617–4626.
- [49] Pintre, I.C.; Gimeno, N.; Serrano, J.L.; Ros, M.B.; Alonso, I.; Folcia, C.L.; Ortega, J.; Etxebarria, J. *J. Mater. Chem.* **2007**, *17*, 2219–2227.
- [50] Pintre, I.C.; Serrano, J.L.; Ros, M.B.; Martínez-Perdiguero, J.; Alonso, I.; Ortega, J.; Folcia, C.L.; Etxebarria, J.; Alicante, R.; Villacampa, B. *J. Mater. Chem.* **2010**, *20*, 2965–2971.
- [51] Vera, F.; Barbera, J.; Romera, P.; Serrano, J.L.; Ros, M.B.; Sierra, T. *Angew. Chem., Int. Ed.* **2010**, *49*, 4910–4914.
- [52] Nair, G.G.; Prasad, S.K.; Hiremath, U.S.; Yelamagad, C.V. *J. Appl. Phys.* **2001**, *90*, 48–53.
- [53] Prasad, S.K.; Nair, G.G.; Sandhya, K.L.; Shankar Rao, D.S. *Mol. Cryst. Liq. Cryst.* **2005**, *436*, 83–105.
- [54] Kim, H.; Kim Lim, T.; Shin, S.T.; Lee, C.K.; Araoka, F.; Ofuji, M.; Takanishi, Y.; Takezoe, H. *Phys. Rev. E* **2004**, *69*, 061701-1–061701-5.
- [55] Lutfur, M.R.; Hegde, G.; Kumar, S.; Tschierske, C.; Chigrinov, V.G. *Opt. Mater.* **2009**, *32*, 176–183.
- [56] Rahman, L.; Kumar, S.; Tschierske, C.; Israel, G.; Ster, D.; Hegde, G. *Liq. Cryst.* **2009**, *36*, 397–408.
- [57] Imrie, C.T.; Henderson, P.A. *Chem. Soc. Rev.* **2007**, *36*, 2096–2124.
- [58] Andersch, J.; Tschierske, C. *Liq. Cryst.* **1996**, *21*, 51–63.
- [59] Zhang, Y.; Martínez-Perdiguero, J.; Baumeister, U.; Walker, C.; Etxebarria, J.; Prehm, M.; Ortega,

- J.; Tschierske, C.; O'Callaghan, M.J.; Harant, A.; Handschy, H. *J. Am. Chem. Soc.* **2009**, *131*, 18386–18392.
- [60] Martinez-Perdiguerro, J.; Zhang, Y.; Walker, C.; Etxeberria, J.; Folcia, C.L.; Ortega, J.; O'Callaghan, M.J.; Baumeister, U. *J. Mater. Chem.* **2010**, *20*, 4905–4909.
- [61] Prasad, S.K.; Sandhya, K.L.; Nair, G.G.; Hirematn, U.S.; Yelamaggad, C.V. *J. Appl. Phys.* **2002**, *92*, 838–841.
- [62] Choi, S.-W.; Izumi, T.; Hoshino, Y.; Takanishi, Y.; Ishikawa, K.; Watanabe, J.; Takezoe, H. *Angew. Chem., Int. Ed.* **2006**, *45*, 1382–1385.
- [63] Mallia, V.A.; Tamaoki, N. *Chem. Mater.* **2003**, *15*, 3237–3239.
- [64] Mallia, V.A.; Funahashi, M.; Tamaoki, N. *J. Phys. Org. Chem.* **2007**, *20*, 878–883.
- [65] Henderson, P.A.; Cook, A.G.; Imrie, C.T. *Liq. Cryst.* **2004**, *31*, 1427–1434.
- [66] Kreger, K.; Wolfer, P.; Audorff, H.; Kador, L.; Stingelin-Stutzmann, N.; Smith, P.; Schmidt, H.-W. *J. Am. Chem. Soc.* **2010**, *132*, 509–516.
- [67] Imrie, C.T.; Henderson, P.A.; Seddon, J.M. *J. Mater. Chem.* **2004**, *14*, 2486–2488.
- [68] Imrie, C.T.; Henderson, P.A.; Yeap, G.-Y. *Liq. Cryst.* **2009**, *36*, 755–777.
- [69] Dantlgraber, G.; Diele, S.; Tschierske, C. *Chem. Commun.* **2002**, 2768–2769.
- [70] Achten, R.; Koudijs, A.; Giesberg, M.; Marcelis, A.T.M.; Sudhölter, E.J.R.; Schröder, M.W.; Weissflog, W. *Liq. Cryst.* **2007**, *34*, 59–64.
- [71] Keith, C.; Amarathana Reddy, R.; Baumeister, U.; Hahn, H.; Lang, H.; Tschierske, C. *J. Mater. Chem.* **2006**, *16*, 3444–3447.
- [72] Keith, C.; Dantlgraber, G.; Amarathana Reddy, R.; Baumeister, U.; Prehm, M.; Hahn, H.; Lang, H.; Tschierske, C. *J. Mater. Chem.* **2007**, *17*, 3796–3805.
- [73] Kosata, B.; Tamba, M.G.; Baumeister, U.; Pelzl, G.; Diele, S.; Pelzl, G.; Galli, G.; Samaritani, S.; Agina, E.V.; Boiko, N.I.; Shibaev, V.P.; Weissflog, W. *Chem. Mater.* **2006**, *18*, 691–701.
- [74] Umadevi, S.; Sadashiva, B.K.; Shreenivasa Murthy, H.N.; Raghunathan, V.A. *Soft Matter* **2006**, *2*, 210–214.
- [75] Umadevi, S.; Sadashiva, B.K. *Liq. Cryst.* **2007**, *34*, 673–681.
- [76] Pelzl, G.; Weissflog, W. In *Thermotropic Liquid Crystals—Recent Advances*, Ramamoorthy, A. ed.; Springer: Dordrecht, The Netherlands, 2007; pp. 1–54.
- [77] Keith, C.; Lehmann, A.; Baumeister, U.; Prehm, M.; Tschierske, C. *Soft Matter* **2010**, *6*, 1704–1721.
- [78] Tschierske, C.; Photinos, D.J. *J. Mater. Chem.* **2010**, *20*, 4263–4294.
- [79] Yelamaggad, C.V.; Prasad, S.K.; Nair, G.G.; Shashikala, I.S.; Rao, D.S.S.; Lobo, C.V. Chandrasekhar, S. *Angew. Chem., Int. Ed.* **2004**, *43*, 3429–3432.
- [80] Prasad, S.K.; Nair, G.G.; Rao, D.S.S.; Lobo, C.V.; Shashikala, I.S.; Yelamaggad, C.V. *Mol. Cryst. Liq. Cryst.* **2005**, *437*, 211–221.
- [81] Yelamaggad, C.V.; Nagamani, S.A.; Hiremath, S.A.; Nair, G.G. *Liq. Cryst.* **2001**, *28*, 1009–1015.
- [82] Jakli, A.; Liao, G.; Shashikala, I.; Hiremath, U.S.; Yelamaggad, C.V. *Phys. Rev. E* **2006**, *74*, 041706–1–041706-6.
- [83] Lee, G.; Jeong, H.-C.; Araoka, F.; Ishikawa, K.; Lee, J.G.; Kaang, K.-T.; Cepic, M.; Takezoe, H. *Liq. Cryst.* **2010**, *37*, 883–892.
- [84] Tamba, M.G.; Kosata, B.; Pelz, K.; Diele, S.; Pelzl, G.; Vakhovskaya, Z.; Kresse, H.; Weissflog, W. *Soft Matter* **2006**, *2*, 60–65.
- [85] Heuer, J.; Stannarius, R.; Tamba, M.-G.; Weissflog, W. *Phys. Rev. E* **2008**, *77*, 056206-1–056206-11.
- [86] Stannarius, R.; Heuer, J. *Eur. Phys. J. E* **2007**, *24*, 27–33.
- [87] Stannarius, R.; Eremin, A.; Tamba, M.-G.; Pelzl, G.; Weissflog, W. *Phys. Rev. E* **2007**, *76*, 061704-1–061704-7.
- [88] Tamba, M.-G.; Baumeister, U.; Pelzl, G.; Weissflog, W. *Liq. Cryst.* **2010**, *37*, 853–874.
- [89] Yelamaggad, C.V.; Shashikala, I.S.; Li, Q. *Chem. Mater.* **2007**, *19*, 6561–6568.
- [90] Bisoyi, H.K.; Srinivasa, H.T.; Kumar, S. *Beilsteins J. Org. Chem.* **2009**, *5*, No. 52-1–52-5.
- [91] Murthy, H.N.S.; Sadashiva, B.K. *J. Mater. Chem.* **2004**, *14*, 2813–2821.
- [92] Rötze, U.; Lindau, J.; Reinhold, G.; Kuschel, F. *Z. Chem.* **1987**, *27*, 293–294.
- [93] Rötze, U.; Lindau, J.; Weissflog, W.; Reinhold, G.; Unseld, W.; Kuschel, F. *Mol. Cryst. Liq. Cryst.* **1989**, *170*, 185–193.
- [94] Pelzl, G.; Diele, S.; Jakli, A.; Weissflog, W. *Liq. Cryst.* **2006**, *33*, 1513–1523.
- [95] Coleman, D.A.; Fernsler, J.; Chattham, N.; Nakata, M.; Takanishi, Y.; Körblova, E.; Link, D.R.; Shao, R.-F.; Jang, W.G.; MacLennan, J.E.; Mondainn-Monval, O.; Boyer, C.; Weissflog, W.; Pelzl, G.; Chien, L.-C.; Zasadzinski, J.; Watanabe, J.; Walba, D.M.; Takezoe, H.; Clark, N.A. *Science* **2003**, *301*, 1204–1211.
- [96] Yu, F.C.; Yu, L.J. *Chem. Mater.* **2006**, *18*, 5410–5420.
- [97] Yu, F.C.; Yu, L.J. *Liq. Cryst.* **2008**, *35*, 799–813.
- [98] Das, B.; Grande, S.; Weissflog, W.; Eremin, A.; Schröder, M.W.; Pelzl, G.; Diele, S.; Kresse, H. *Liq. Cryst.* **2003**, *30*, 529–539.
- [99] Stannarius, R.; Li, J.; Weissflog, W. *Phys. Rev. Lett.* **2003**, *90*, 025502-1–025502-4.
- [100] Sarkar, G.; Das, M.K.; Paul, R.; Das, B.; Weissflog, W. *Phase Transitions* **2009**, *82*, 433–443.
- [101] Han, X.F.; Wang, S.T.; Cady, A.; Liu, Z.Q.; Findeisen, S.; Weissflog, W.; Huang, C.C. *Phys. Rev. E* **2003**, *68*, 060701–060704.
- [102] Sarkar, G.; Das, B.; Das, M. K.; Baumeister, U.; Weissflog, W. *Mol. Cryst. Liq. Cryst.* **2011**, *540*, 188–195.
- [103] Enz, E.; Findeisen, S.; Dabrowski, R.; Giesselmann, F.; Weissflog, W.; Baumeister, U.; Lagerwall, J. *J. Mater. Chem.* **2009**, *19*, 2950–2957.
- [104] Nishiyama, I.; Goodby, J.W. *J. Mater. Chem.* **1992**, *2*, 1015–1023.
- [105] Gasowska, J.; Dabrowski, R.; Filipowicz, M.; Predmojski, J. *Ferroelectrics* **2006**, *343*, 61–67.
- [106] Gasowska, J.; Dabrowski, R.; Drzewinski, W.; Kenig, K.; Tykarska, M.; Predmojski, J. *Mol. Cryst. Liq. Cryst.* **2004**, *411*, 231–241.
- [107] Wang, S.T.; Wang, S.L.; Han, X.F.; Liu, Z.Q.; Findeisen, S.; Weissflog, W.; Huang, C.C. *Liq. Cryst.* **2005**, *32*, 609–617.
- [108] Chakraborty, A.; Das, B.; Das, M.K.; Findeisen-Tandel, S.; Tamba, M.-G.; Baumeister, U.

- Kresse, H.; Weissflog, W. *Liq. Cryst.* **2011**, *38*, 1085–1097.
- [109] Pelzl, G.; Schiller, P.; Demus, D. *Liq. Cryst.* **1987**, *2*, 131–148.
- [110] Naito, T.; Horie, K.; Mita, I. *Macromolecules* **1991**, *24*, 2907–2911.
- [111] Tateishi, Y.; Tanaka, K.; Nagamura, T. *J. Phys. Chem. B* **2007**, *111*, 7761–7766.
- [112] Shibaev, V.; Medvedev, A.; Bobrovsky, A. *J. Polym. Sci., A: Polym. Chem.* **2008**, *46*, 6532–6541.
- [113] Kasha, M.; Rawls, H.R.; El-Bayoumi, M.A. *Pure Appl. Chem.* **1965**, *11*, 371–392.
- [114] Chigrinov, V.; Pikin, S.; Verevochnikov, A.; Kozenkov, V.; Khazimullin, M.; Ho, J.; Huang, D.D.; Kwok, H.-S. *Phys. Rev. E* **2004**, *69*, 061713-1–061713-10.